Chapter Eight

Controlling Infectious Diseases

One of the important uses of epidemiological models is to provide some basic guidelines for public health practitioners. Models have two primary uses in applied settings. First, as we have seen in previous chapters, statistical data analyses and model fitting permit basic epidemiological characteristics of pathogens to be uncovered. This, in conjunction with empirical observations, enables epidemiologists to develop a picture of the kind of pathogen they are faced with, such as its transmission potential, routes of transmission, and latent and infectious periods. The second use of epidemiological models is to provide a means of comparing the effectiveness of different potential management strategies.

The most straightforward objective is simply to minimize *transmission* within a population, with the ultimate aim of reducing it to zero. Alternatively, we may wish to minimize the occurrence of *disease* (or severe illness). Although for many infectious diseases these two objectives may amount to the same control outcomes, for others this change in emphasis can have dramatic implications for control strategies. For example, infectious diseases such as rubella are associated with minimal health risks when affecting the young or the old, whereas infection in pregnant women can have very serious consequences (Behrman and Krliegman 1998). This age-dependent severity has a profound impact on which control strategies are optimal (see later for a full exposition).

In reality, a range of constraints and trade-offs may substantially influence the choice of practical control strategy, and therefore their inclusion in any modeling analysis may be important. These limitations may be simply logistical, in terms of the number of units of vaccine that can be administered in a given time frame, or epidemiological such as adverse reactions to a vaccine. Frequently, epidemiological models need to be coupled to economic considerations, such that control strategies can be judged through holistic cost-benefit analyses (see, for example, Michael et al. 2004). Control of livestock diseases is a scenario when cost-benefit analysis can play a vital role in choosing between cheap, weak controls that lead to a prolonged epidemic, or expensive but more effective controls that lead to a shorter outbreak. For human diseases, cost-benefit analysis may still be applied, but its interpretation is more subjective (see, for example, Hay and Ward 2005).

When attempting to model epidemics and control for public-health applications, there is the compelling urge to make models as sophisticated as possible, including many details of the host and pathogen biology. Although this strategy may be beneficial when such details are known or there exist adequate data to parameterize the model, it may lead to a false sense of accuracy when reliable information is not available. In general, we believe it is better to start with simple models that can provide a generic understanding and then investigate systematically the effects of adding more complexity or detail—this is the approach advocated throughout this book. In addition, it is also important that any detailed model is accompanied by a sensitivity analysis of the assumptions and parameters, without which it is difficult to ascertain the reliability of any predictions.

Despite the assertion that simple models are required to generate a deeper understanding of many issues associated with control, it will become obvious that the models in this chapter are more complex and parameter-rich than those in previous chapters. In general, as we move toward models that are more applied in nature, we encounter a proliferation of parameters necessary to capture the many aspects of transmission and control that are thought to be important. This has two main implications: (1) it is more difficult to obtain a general understanding of the model behavior across all parameter space; and (2) careful, statistically rigorous, parameterization of the model from detailed data becomes ever more important. Finally, even though the models in this chapter are among the most complex in the book, they are still relatively simple compared to some of the sophisticated public health and veterinary models that are used.

In this chapter, we review some mathematical models for different types of control strategies available to decision makers, with some of their inherent limitations and the general principles that emerge from their analyses. We start by considering alternative aspects of vaccination, then move on to controlling infections by reducing transmission opportunities via contact tracing and quarantine methods. Finally, we discuss two case studies, one that highlights the need for a combination of vaccination and contact reduction, and another that demonstrates the importance of seasonality and density-dependent factors in determining the optimal culling of wildlife populations.

8.1. VACCINATION

Perhaps the best documented example of infectious disease management has been the exploration of the levels of prophylactic vaccination necessary for eradication. Since the pioneering work of Edward Jenner on smallpox (Fenner et al. 1988), the process of protecting individuals from infection by immunization has become routine, with substantial historical successes in reducing both mortality and morbidity. Typically, vaccines contain antigens, which are either the whole- or broken-cell protein envelopes from the virus or bacterium causing a specific disease. When efficacious, the presence of such antigens illicits an immune response in the host, intended to be similar to the consequences of actual infection. The assumption (and hope) is that the vaccine provides long-lasting immunity to the infection, preventing both *transmission* and *disease*.

Two forms of random vaccination are possible: The most common for human diseases is pediatric vaccination to reduce the prevalence of an endemic disease; the alternative is random vaccination of the entire population in the face of an epidemic—such a policy of mass-vaccination may be applied in case of any potential smallpox outbreak (see Section 8.1.2).

8.1.1. Pediatric Vaccination

For many potentially dangerous human infections (such as measles, mumps, rubella, whooping cough, polio, etc.), there has been much focus on vaccinating newborns or very young infants. The mathematical treatment of this practice is wonderfully straightforward and requires making a single addition to the $S(E)IR$ equations. Conventionally, the parameter p is used to denote the fraction of newborns (or infants who have lost any maternally derived immunity) who are successfully vaccinated and are therefore "born" into the immune class. This term, p, is the product of the actual vaccination *coverage* (the percentage of newborns who receive the required number of vaccine doses) and the vaccine

efficacy (the probability that they successfully develop immunity). When incorporated into the SIR system, we get the following set of modified equations:

This is online program 8.1

$$\begin{aligned}\frac{dS}{dt} &= \nu(1-p) - \beta IS - \mu S,\\ \frac{dI}{dt} &= \beta SI - (\gamma+\mu)I,\\ \frac{dR}{dt} &= \gamma I + \nu p - \mu R.\end{aligned} \tag{8.1}$$

This modification can be dynamically explored using a simple (linear) change of variables: $S = S'(1-p)$, $I = I'(1-p)$, and $R = R'(1-p) + \frac{\nu}{\mu}p$ (Earn et al. 2000). These substitutions give rise to a new set of ODEs:

$$\begin{aligned}\frac{(1-p)dS'}{dt} &= \nu(1-p) - (\beta I'(1-p)+\mu)S'(1-p),\\ \frac{(1-p)dI'}{dt} &= \beta S'I'(1-p)^2 - (\gamma+\mu)I'(1-p),\\ \frac{(1-p)dR'}{dt} &= \gamma I'(1-p) + \nu p - \mu R'(1-p) - \nu p.\end{aligned} \tag{8.2}$$

Clearly, these equations can be simplified by cancelling out the terms $(1-p)$ on both sides. This gives:

$$\begin{aligned}\frac{dS'}{dt} &= \nu - (\beta(1-p)I' + \mu)S',\\ \frac{dI'}{dt} &= \beta(1-p)S'I' - (\gamma+\mu)I',\\ \frac{dR'}{dt} &= \gamma I' - \mu R'.\end{aligned} \tag{8.3}$$

After some thought, it becomes obvious that these equations (8.3) are identical to the basic SIR equations with a single important modification: The transmission rate β is replaced with $\beta(1-p)$. Note that if, instead of vaccination, we were attempting to deal with the dynamical consequences of a systematic change in the per capita birth rates (from ν to ν', for instance), then we would instead replace β with $\beta\frac{\nu'}{\nu}$. These observations simply translate into the following general conclusion:

A system either subject to constant long-term vaccination of a fraction p of newborns against an infection with a basic reproductive ratio R_0, or with a modified per capita birth rate of ν', is dynamically identical to a system with $R_0' = (1-p)\frac{\nu'}{\nu}R_0$.

Although this vaccination result is simple, it is also very powerful. In order to eradicate a pathogen by long-term pediatric vaccination, we need to ensure that the fraction of susceptible individuals in the population is sufficiently small to prevent the spread of the infection (i.e., $dI/dt \le 0$). This is effectively the threshold theorem of Kermack and McKendrick (1927) and means we need to ensure $R_0' = (1-p)R_0 < 1$, which translates into vaccinating a critical proportion of the newborns

$$p_c = 1 - 1/R_0. \tag{8.4}$$

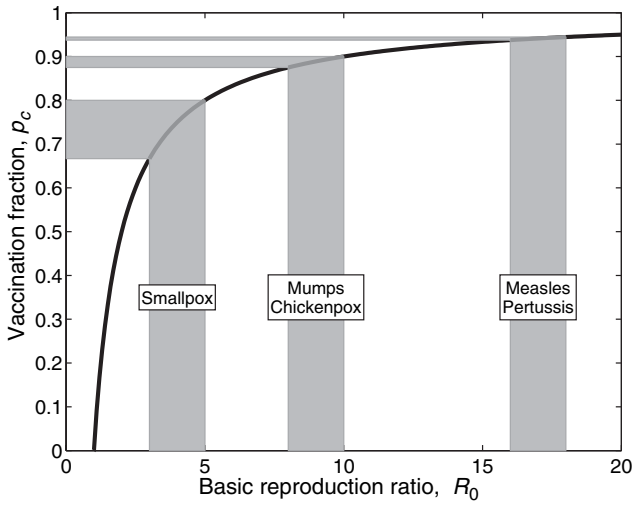

Figure 8.1. The critical fraction of newborns that must be vaccinated to eradicate an infection with a specific basic reproductive ratio (R_0). The figure demonstrates that all incoming susceptibles need not be vaccinated to ensure the infection is not endemic. The shaded regions show the range of p_c for the estimated R_0 of different infections.

This vaccination threshold make good intuitive sense, demonstrating that greater action is required for infectious diseases with a larger basic reproductive ratio. The relationship between p_c and R_0 is plotted in Figure 8.1. It demonstrates that for diseases with very high transmission potential, such as measles and pertussis (R_0 between 16 and 18; Anderson and May 1982), the vaccinated fraction of newborns needed for eradication is somewhere between 93% and 95%. For mumps and chickenpox, on the other hand, the threshold vaccination level is lower, ranging from 87.5% to 90%. For smallpox, p_c was below 80%. To date, smallpox is the only high-profile example of global eradication of a potentially fatal infection. In recent years, there has been a tendency to credit its elimination to a policy of surveillance, containment, and ring vaccination (intensive immunization of individuals in the vicinity of a known case—more below) in the mid- to late-1970s. This misses the point, however, that background vaccination is likely to have sufficiently reduced transmission within the population to such a level that ring vaccination was able to successfully target the remaining susceptibles (Arita et al. 1986).

In order to eradicate an infection, not all individuals need to be vaccinated, as long as a critical proportion (determined by the reproductive ratio of the infection) have been afforded protection. This phenomenon is referred to as "herd immunity" (Fine 1993).

Vaccinating at the critical level p_c does not instantly lead to eradication of the disease. The level of immunity within the population requires time to build up and at the critical level it may take a few generations before the required herd immunity is achieved. Thus, from a public health perspective, p_c acts as a lower bound on what should be achieved, with higher levels of vaccination leading to a more rapid elimination of the disease.

However, the converse is also true. Vaccination is still a worthwhile control measure even when the critical level cannot be achieved. In such cases, vaccination reduces the prevalence of infection:

$$I^* = \frac{\nu(1-p)}{(\gamma+\mu)} - \frac{\mu}{\beta}. \tag{8.5}$$

Hence, the equilibrium fraction of infecteds decreases linearly with increasing vaccination, until eradication is achieved. Thus, even limited vaccination provides protection at the population level, as well as direct protection for those individuals vaccinated. Comparing equation (8.5) with the unvaccinated equilibrium ($I^* = \nu/(\gamma+\mu) - \mu/\beta$; see Chapter 2), we see that $\mu p/\beta$ unvaccinated individuals are saved from infection due to the herd-immunity effects.

Additionally, the stochastic nature of disease transmission can contribute to the beneficial effects of limited vaccination. Consider equation (8.1); in terms of the transmission process, a vaccinated population is similar to a smaller population (of size $(1-p)N$) with a reduced basic reproductive ratio. The effective reduction in R_0 leads not only to lower prevalence, as outlined above; this also enhances the effects of stochasticity and can lead to chance extinction. Thus, even when vaccination does not exceed the deterministic threshold, eradication may occur; the chain of transmission can be broken by chance (see Section 6.3.3.3). However, because the level of control is below the critical threshold, the disease can re-invade after a stochastic extinction, leading to subsequent epidemics.

These principles are illustrated in Figure 8.2. The straight gray line shows how the number of infecteds within the population can be reduced even when vaccinating below the eradication threshold. The black lines are the average time to extinction, taken as the time from the onset of vaccination (when the population is assumed to be at the unvaccinated equilibrium) until the infection undergoes stochastic extinction and is eradicated from the population. This extinction time illustrates three important points: First, when vaccinating at birth, it always takes time to eradicate an infectious disease, even when the vaccination is well above the threshold p_c. Second, eradication can occur below the vaccination threshold due to either stochastic effects or the deep trough in the number of infecteds that accompanies the sudden onset of vaccination (the "honeymoon period," as termed by McLean 1995). Finally, population size plays an overwhelming role; it is only for the very highest levels of vaccination that the large (one million individuals) population is driven extinct as rapidly as the unvaccinated small (100,000 individuals) population.

One of the obvious consequences of the reduced frequency of disease transmission is that those (unvaccinated) individuals who eventually contract the infection are likely to be older than in the absence of vaccination. It is straightforward to derive an expression for the mean age at infection in the SIR model with vaccination (A') as a function of the mean age at infection for an unvaccinated population (A):

$$A' = A/(1-p).$$

As we discussed in Chapter 5 an important implication of this result is that we can produce a single bifurcation diagram that summarizes the *dynamics* of an infectious disease as vaccination or demographic rates systematically vary. This means that we may think of a system under vaccination as dynamically equivalent to a system with a proportionately reduced R_0. As mentioned in Chapter 5, this argument may be somewhat complicated by

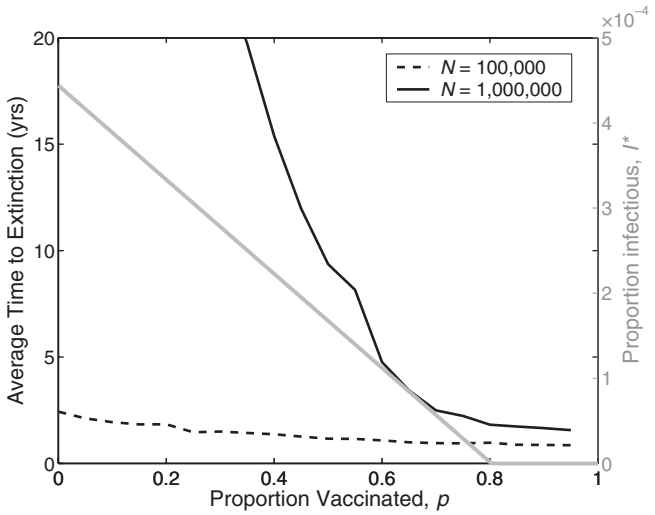

Figure 8.2. The effects of vaccinating a proportion p of the population at birth in a stochastic model. We consider host population sizes of 10^5 and 10^6, and start the simulations with the population at the unvaccinated equilibrium point. The gray line shows the mean prevalence of infection after vaccination, as predicted by equation (8.5). The black curve shows the average time to "extinction" (also called the "first passage time") measured from the start of vaccination. (Model parameters were $\mu = 0.02$ per year, $R_0 = 5$, $1/\gamma = 5$ days.)

changes in the strength of seasonality in transmission because the mean age at infection increases following immunization.

8.1.2. Wildlife Vaccination

There are many instances, especially for wildlife diseases or perhaps when vaccine boosters are necessary, where control by vaccination means targeting the entire susceptible pool and not just the newborns. This can occur through distributing feed containing vaccine (e.g., to control rabies in foxes), or administering vaccines (e.g., to control distemper in domestic dog populations). In such cases, we model the random vaccination of any member of the population (irrespective of disease status), although it is only the vaccination of susceptible individuals that has any effect. The vaccination parameter, v, now necessarily becomes a *rate* rather than a *fraction* and we are concerned with the proportion of the susceptible population immunized per unit time. The changes in the mathematical equations describing this scenario are small:

$$\begin{aligned} \frac{dS}{dt} &= \mu - (\beta I + \mu - v)S, \\ \frac{dI}{dt} &= \beta SI - (\gamma + \mu)I, \\ \frac{dR}{dt} &= \gamma I + vS - \mu R. \end{aligned} \tag{8.6}$$

This is online program 8.2

The dynamical consequences of this introduction are qualitatively minor. The system still possesses two equilibria, one that is disease free and another with the infection endemic. The primary difference is that we now need to evaluate the vaccination *rate* required to eliminate the infection. After some algebra, we find the critical rate of vaccination, $v_c = \mu(R_0 - 1)$. This criterion is clearly different in structure to that derived from equation (8.2). Here, v_c increases linearly with R_0 rather than the previously concave relationship. In actuality, however, these two thresholds (p_c and v_c) lead to the same fraction of the population needing to be vaccinated in order to eliminate the infection. At the critical threshold, a fraction $v_c S^*$ are vaccinated daily; substituting for the values gives $\frac{1}{R_0} \times \mu(R_0 - 1)$, which simplifies to $\mu(1 - 1/R_0) = \mu p_c$, as derived in Section 8.1.1. Therefore, these two vaccination schemes are equivalent in terms of the *numbers* of susceptible hosts who need to be immunized. The key practical difference, however, lies in the fact that wildlife vaccination assumes that the fraction of the population susceptible to infection (given by $1/R_0$) cannot be unambiguously identified and therefore vaccination effort is spread across the entire population—even though it is effective only for susceptible animals. For this reason, regulating an infectious disease by reducing the recruitment of individuals susceptible to it (equation (8.1)) may be perhaps easier than attempting to immunize the susceptible population (equation (8.6)).

8.1.3. Random Mass Vaccination

For rare, nonendemic pathogens, continual vaccination at birth is not a cost-effective control measure. Instead, a mass-vaccination program may be initiated whenever there is increased risk of an epidemic. In such situations there is a "race" between the exponential increase of the epidemic, and the logistical constraints upon mass-vaccination. For most human diseases it is possible (and more efficient) to record who has been vaccinated, and only immunize those who have not received the vaccine—an even more refined approach would not vaccinate those individuals who have recovered from the disease because they are already protected. We take as our most simple model:

$$\begin{aligned} \frac{dS}{dt} &= -\beta SI - u, \\ \frac{dI}{dt} &= \beta SI - \gamma I, \\ \frac{dR}{dt} &= gI, \\ \frac{dV}{dt} &= u, \end{aligned} \tag{8.7}$$

where demographics have been ignored because we are primarily interested in the short-term response to an emerging epidemic or pandemic. We obviously insist that vaccination stops once the number of susceptibles reaches zero. Two extremes of this model can be considered. When u is small, vaccination will have little impact on the epidemic and a proportion R_∞ of the population will be infected ($R_\infty = 1 - \exp(-R_0 R_\infty)$; Chapter 2). At the other extreme, when u is large we can use the approximation $S(t) \approx max(S(0) - ut, 0)$, which assumes that the level of susceptibles is decreased by vaccination although the impact of infection on the level of susceptibles is insignificant and ignored. This is a reasonable assumption if the rate of vaccination is sufficient to control the outbreak. Under

these assumptions, the number of infectious cases is given by:

$$I(t) \approx \begin{cases} I(0)\exp\left(\left[\beta S(0) - \gamma - \frac{1}{2}\beta u t\right] t\right) & t \leq \dfrac{S(0)}{u} \\ I(0)\exp\left(\frac{1}{2}\beta S(0)^2/u - \gamma t\right). & \text{otherwise} \end{cases}$$

Here, the fraction of infecteds follows a Gaussian curve, and the initial disease prevalence at the onset of immunization ($I(0)$) determines the scale of the ensuing epidemic. This conclusion echoes a broad tenet in epidemiology, that the best way to control an epidemic is to hit it hard and hit it early—a strong response leads to the fastest reduction in the susceptible population, which in turn reduces the epidemic, and a rapid response prevents the exponential increase of cases from getting beyond logistical control.

8.1.4. Imperfect Vaccines and Boosting

Despite the effectiveness of vaccines in dramatically reducing the number of new infectious cases (and the severity of illness), the resurgence and epidemic outbreaks of some infectious diseases are considered to be of major public health concern (Orenstein et al. 2004). Among childhood infections, measles is a well-known candidate for such outbreaks and still contributes to over one million deaths annually, mostly among children in developing countries. Clinical studies have proposed several potential explanations, including decreased immunization coverage together with irregularities in the supply of vaccines, incomplete protection conferred by imperfect vaccines, and the loss of vaccine-induced immunity (Garly and Aaby 2003; Janaszek et al. 2003).

To prevent an endemic spread of measles infection, many countries, mostly in the developed world, have revised their vaccination programs to include multiple schedules. The reported clinical data using the strategy of a booster MMR (measles-mumps-rubella) vaccine confirm that these countries have generally succeeded in controlling the spread of infection. Hence, in order to achieve a global eradication, the World Health Organization recommends a booster vaccination program worldwide. The central question to ask is whether this strategy could eventually provide the conditions for global eradication. To address this question, we can develop a framework, modified from the $SEIR$ equations, that would predict the consequences of the introduction of a booster schedule, in terms of the known major factors associated with a vaccination program (McLean and Blower 1993; Gandon et al. 2001, 2003).

The model we present is due to Alexander et al. (2006) and is composed of four distinct classes: Susceptible (S), Vaccinated (S_v), Infectious (I), and Booster vaccinated (or recovered) individuals (V) who are immune for life. It accounts for two major aspects of an imperfect vaccine: (1) incomplete protection, and (2) waning of vaccine-induced immunity. The first may result in the subsequent infection of the pediatric-vaccinated class, perhaps at a lower rate than that of the fully susceptible class. The second leads to an increase in the size of the fully susceptible pool through the loss of vaccine-induced immunity. The model also assumes that, like the natural immunity induced by the infection, the booster vaccine administered to the class of pediatric-vaccinated individuals confers complete protection against the disease. The system can be mathematically expressed by the following system of differential equations:

$$\frac{dS}{dt} = (1-p)\mu - \beta SI - \mu S - \xi S + \delta S_v, \tag{8.8}$$

$$\frac{dS_v}{dt} = p\mu + \xi S - (1-\alpha)\beta S_v I - (\mu + \rho + \delta)S_v, \tag{8.9}$$

$$\frac{dI}{dt} = \beta SI + (1-\alpha)\beta S_v I - (\mu + \gamma)I, \tag{8.10}$$

$$\frac{dV}{dt} = \rho S_v + \gamma I - \mu V, \tag{8.11}$$

where p is the fraction of newborns who receive the pediatric vaccine, α represents the efficacy of the vaccine in terms of reducing the susceptibility of (singly) vaccinated individuals, δ is the waning rate following pediatric vaccination, $1/\gamma$ is the infectious period, μ is the natural death rate, and ρ and ξ are the rates of administration of the booster vaccine to previously vaccinated and susceptible individuals, respectively.

As demonstrated in Chapter 3, by studying the dominant eigenvalues of these equations, we can derive the effective reproductive ratio, r_0, which is defined here as the number of secondary cases resulting from a single index case given the specified vaccination regime (Alexander et al. 2006). We get the following expression:

$$r_0 = \frac{\mu[\delta + (1-p)(\mu+\rho) + (\mu p + \xi)(1-\alpha)]\beta}{(\mu+\gamma)[(\mu+\xi)(\mu+\rho) + \mu\delta]}. \tag{8.12}$$

Naturally, there is significant public health interest to ensure control parameters that would make eradication feasible by reducing r_0 below unity. An increase in μ, δ, or β—which relate to more susceptibles entering the population, a decrease in the mean duration of vaccine-induced immunity, and a higher transmission rate respectively —can all be offset by a higher level of pediatric vaccination. It is useful to rewrite equation (8.12) in terms of the basic reproductive ratio for a population that is wholly susceptible, with no vaccination (R_0). This gives:

$$r_0 = \left(1 - \frac{(\mu p + \xi)(\rho + \mu\alpha)}{(\mu+\rho)(\mu+\xi) + \mu\delta}\right) R_0, \tag{8.13}$$

where, as before, $R_0 = \beta/(\mu+\gamma)$. Clearly, a high value of R_0 requires a high coverage level of pediatric vaccination, p, to prevent the spread of the infectious disease, regardless of the type of vaccine being administered. However, it is practically unfeasible to vaccinate all individuals in the susceptible class (p is always significantly less than 1), particularly in countries where finances play a major role in the number of people who receive the vaccines. Hence, the next best strategy is to determine the critical number needed to be vaccinated and try to achieve this value.

It is instructive to establish the minimum pediatric vaccination level that is required to eliminate the infectious disease in the absence of boosters ($\rho = \xi = 0$)—the equivalent to the standard vaccination model but with waning immunity and partial protection. This is given by:

$$p_c = \left(1 - \frac{1}{R_0}\right)\left(\frac{\mu+\delta}{\mu\alpha}\right), \tag{8.14}$$

such that $r_0 \leq 1$ whenever $p \geq p_c$. Not surprisingly, this threshold reduces to $p_c = 1 - 1/R_0$ for a perfect vaccine ($\alpha = 1,\ \delta = 0$). The most important implication of this result is that eradication may be impossible to achieve once the basic reproductive ratio, R_0, is

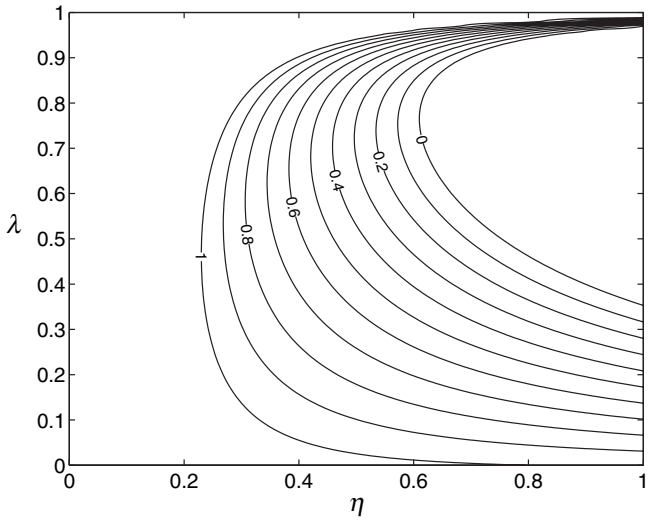

Figure 8.3. Contour plots for various values of critical pediatric vaccination coverage, p_c, as the total rate of booster vaccination, η, and the proportion of booster vaccination given to unvaccinated individuals, λ. These two quantities can be related to those in equations (8.8)–(8.11) as $\xi = \lambda\eta$ and $\rho = (1-\lambda)\eta$. The critical values of p are found by setting r_0 in equation (8.12) to one. (Parameter values are: $1/\mu = 50$ years, $1/\delta = 20$ years, $\alpha = 0.95$, and $1/\gamma = 14$ days.)

greater than 2. Consider the optimistic case in which the pediatric vaccine provides perfect immunity to infection ($\alpha = 1$), but where protection wanes through time ($\delta > 0$). In this scenario, equation (8.14) means that the critical proportion of the population required to be vaccinated becomes greater than 1 ($p_c \geq 1$), unless the ratio of life expectancy to the period of protection ($(\mu+\delta)/\mu$) is less than $R_0/(R_0-1)$. As a result, for a pathogen with effective $R_0 = 3$, this result effectively means that eradication requires the period of protection to last for at least $2/3$ the duration of life—hence the need for booster vaccination.

We now introduce a new parameter η as the rate of total booster administration, and let $\xi = \lambda\eta$ and $\rho = (1-\lambda)\eta$ where $0 \leq \lambda \leq 1$. (Note that changing λ but keeping η constant does not imply the vaccination of a constant number of individuals, but a constant vaccination effort partitioned between the two classes.) Let $p_c(\eta, \lambda)$ represent the curve on which $r_0 \equiv 1$ and therefore the minimum level of pediatric vaccination needed to eradicate the infection. Examining the control of an infection such as measles, we set $R_0 = 17$ and show in Figure 8.3 contour plots of $p_c(\eta, \lambda)$ (for feasible ranges of η and λ). For each p_c, there is a critical value η_p (corresponding to a vertical tangent to p_c in Figure 8.3) such that disease control is not feasible if $\eta < \eta_p$. However, for $\eta > \eta_p$, there is a range of λ for which $r_0 < 1$ and the disease can be eradicated. Decreasing the pediatric vaccination coverage p makes the feasible range of λ shrink, with the lower limit of the range showing the greatest change. An important epidemiological consequence of this result is that, for relatively low vaccine coverage (p), a booster program may fail to control the disease if it is mostly targeted to primary vaccinated individuals (λ is too low). The same conclusion can be derived when λ is too high and the booster in effect functions mostly as primary vaccination. More important, the probability of failure of a booster program increases as

pediatric vaccination coverage p decreases, leading to a more restricted range of λ for disease control. This highlights the significant role that primary coverage plays in ensuring a successful booster program (Alexander et al. 2006).

In this section, we have considered the impact of imperfect vaccines in reducing the basic reproductive number. We have used a slightly modified SIR framework to evaluate the effect of a booster dose of an imperfect vaccine, to supplement primary vaccination, in reducing R_0. Our findings highlight two important epidemiological messages:

In high incidence areas, eradication with a single dose of imperfect vaccine will be impossible unless the mean period of protection afforded by the vaccine is greater than the average life expectancy multiplied by $1 - 1/R_0$.

Eradication by administering a booster vaccination is feasible only if a minimum rate is achieved.

In addition, infections that require a booster vaccine highlight an important role for models in public health. For a perfect vaccine, the obvious public health initiative is to vaccinate as many individuals as possible; models do little to enhance this response other than define the threshold level—although vaccination at levels above the threshold is still desirable because it speeds eradication. In contrast, when booster vaccines are required there is a clear trade-off in the partitioning of resources between primary and booster vaccination campaigns. Models can help to optimize this trade-off.

If such models were to be used in a public health context, then we would potentially require far greater realism. In particular, it may be necessary to include age structure into the model formulation as well as introduce a more refined description of the time scale of waning immunity (Chapter 3).

8.1.5. Pulse Vaccination

The approaches outlined above are based on the immunization of newborns or relatively young individuals and although the details are population and disease specific, theory generally predicts successful eradication if vaccine-induced immunity levels exceed 70–95% (see, for example, Figure 8.1). Achieving such high levels of coverage presents a daunting challenge, however, especially in the face of financial, political, and logistical difficulties.

An alternative approach that has been tried in a variety of locations is pulse vaccination, where children in certain age cohorts are periodically immunized (Agur et al. 1993; Nokes and Swinton 1997; Shulgin et al. 1998). The rationale for this idea is as follows: The prevalence of an infectious disease increases only if $S \times R_0 > 1$, where S is the fraction of the population that is susceptible. Hence, as demonstrated earlier in this chapter, for any specified infectious agent, there is a critical proportion of susceptibles, $S_c = 1/R_0$, below which spread is unlikely. The principle aim of pulse vaccination is to ensure the susceptible fraction is maintained below this level by periodically immunizing a fraction of the susceptible population. These ideas can be best illustrated by example. Assuming a disease has an R_0 of 10, then, in the long run, 10% of the population will be susceptible on average. If a percentage $p_V = 60\%$ of susceptibles are vaccinated in a single pulse, then only 4% of the population will remain susceptible. Given a per capita birth rate (ν) of 2% per year and a constant population size, it will take 3 years for S to reach 10%, thus providing a crude approximation to the period between pulses (Nokes and Anderson 1988). Pulse vaccination has gained in prominence as a result of its highly successful

application in the field. Compared to "continual" pediatric vaccination, it has the additional advantage that it is often logistically simpler to implement. A well-publicized example is the spectacular control of poliomyelitis and measles in Central and South America (Sabin, 1991; de Quadros et al. 1996).

The theoretical challenge of pulse vaccination is the a priori determination of the pulse interval for specified values of R_0, the vaccination fraction p_V, and population birth rate μ. Simulation methods used by Agur et al. (1993) demonstrated that the optimal pulsing period was approximately equal to the mean age at infection. To make this more rigorous, Shulgin et al. (1998) examined the following refinement of the SIR system:

This is online program 8.3

$$\frac{dS}{dt} = \mu - \beta SI - \mu S - p_V \sum_{n=0}^{\infty} S(nT^-)\delta(t - nT), \tag{8.15}$$

$$\frac{dI}{dt} = \beta SI - \gamma I - \mu I, \tag{8.16}$$

where T is the interval between pulses and $S(nT^-)$ represents the level of susceptibles in the instant immediately prior to the n^{th} vaccination pulse ($n = 0, 1, \ldots$). $\delta(t)$ is the Dirac delta function which is zero unless $t = 0$; hence, the final term in equation (8.15) ensures that the number of susceptibles is reduced by a fraction p_V at every vaccination pulse. We can now establish the optimal pulsing period by studying the disease-free equilibrium and the conditions required for its stability. Leaving aside the details of this stability analysis, which are complicated by the pulses, we arrive at the optimal gap between pulses to ensure eradication as determined by Shulgin et al. (1998):

$$\frac{(\mu T - p_V)(e^{\mu T} - 1) + \mu p_V T}{\mu T(p_V - 1 + e^{\mu T})} < \frac{1}{R_0}. \tag{8.17}$$

This equation can be solved numerically in order to obtain the threshold value of T_c. In Figure 8.4, we plot the value of T_c for three different R_0 values as p_V is varied. It demonstrates that the pulse interval increases with the vaccination fraction and declining R_0. It also shows that in contrast to the numerically obtained estimates by Agur et al. (1993), the values of T_c can exceed the mean age at infection A. The above approximation has been shown to remain good for the $SEIR$ model (d'Onofrio, 2002).

If, as is the case with childhood infections, transmission varies substantially depending on season (see Chapter 5), then we set $\beta(t) = \beta_0(1 + \beta_1 \cos(2\pi t + \psi_0))$, where ψ_0 represents the phase of seasonal transmission for the susceptible population assuming the year starts after a vaccination pulse. Taking this framework, Shulgin et al. (1998) again used stability analysis to show that T_c satisfies:

$$\frac{\big((\mu T - p_V)(e^{\mu T} - 1) + \mu p_V T\big)}{\mu T(p_V - 1 + e^{\mu T})} + \frac{\beta_1 p_V}{T} \frac{(2\pi \sin(\psi_0) - \mu \cos(\psi_0))}{(4\pi^2 + \mu^2)(p_V - 1 + e^{\mu T})} = \frac{1}{R_0}. \tag{8.18}$$

Clearly, the first term in the inequality is simply the unforced case given by inequality (8.17). What we need to examine, therefore, is how much the second term alters the predictions of the constant transmission model. Upon substituting conventional measles parameter values into the above two terms, we find the ratio between the first and the second to be approximately $50 : 1$. Hence, the optimal timing of pulse vaccination is not substantially altered when seasonality is taken into account. It is interesting to note that T_c is affected by the phase shift, with a maximum at $\psi_0 \cong 3\pi/2$ for parameter values

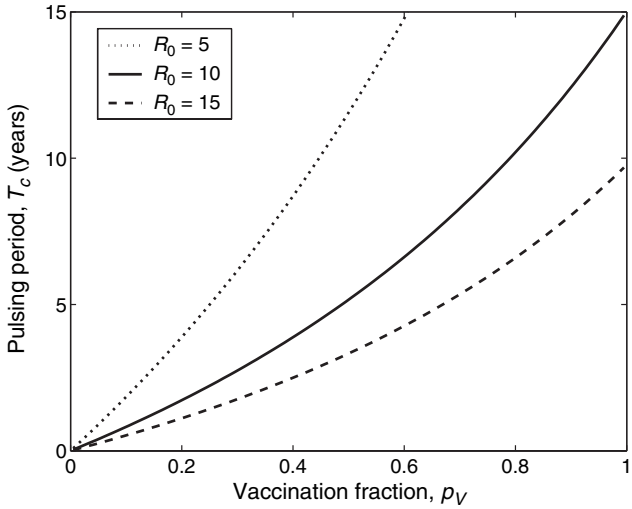

Figure 8.4. The threshold pulsing period (T_c) as a function of the vaccination proportion (p_V) for three different basic reproductive ratios. The curves were generated assuming $1/\mu = 70$ years ($\mu \approx 0.0143$).

representative of measles dynamics. Hence, pulses of vaccination should ideally be applied 3 months after the peak in the seasonal transmission rate $\beta(t)$.

In most countries, pediatric immunization programs are already established and any attempt at pulse vaccination is likely to be *in addition to* constant background vaccination (with probability p) rather than an alternative. Shulgin et al. (1998) demonstrated that the introduction of an additional term to equation (8.15) to take this component into account changes T_c in a very predictable way. The new optimal pulsing period is simply the previously derived value (T_c) divided by $(1 - p)$.

An additional advantage of pulse vaccination becomes apparent when infection is considered in a spatial context (see Section 7.2.3 and Figure 7.5 in Chapter 7). We first note that in England and Wales there was little noticeable decrease in measles persistence following the onset of vaccination at around 60% in the late 1960s—in direct contrast to the predictions from simple mathematical models. It is hypothesized that this surprising observation is due to greater asynchrony of epidemic cycles between communities after vaccination, which in turn means that recolonisation of disease-free populations is enhanced. Pulse vaccination may counter this effect, because the regular decrease in susceptibles due to vaccination may act to synchronize epidemics such that all communities experience troughs at similar times, reducing the chance of recolonization (Earn et al. 1998).

8.1.6. Age-Structured Vaccination

The above models have all ignored the effects of age structure on the vaccination policy. Here, we use the simplest transmission assumption, that the force of infection is independent of age, to consider the optimal age of vaccination.

Consider the scenario when a proportion p of the population are vaccinated at age A_v. The equations for the age-structured population are best considered as two separate sets of identical equations but with different boundary conditions:

$$\begin{aligned} \frac{\partial S(a)}{\partial t} &= -\beta S(a)\widehat{I} - \mu S(a) - \frac{\partial S(a)}{\partial a} \\ \frac{\partial I(a)}{\partial t} &= \beta S(a)\widehat{I} - \gamma I(a) - \mu I(a) - \frac{\partial I(a)}{\partial a}, \end{aligned} \tag{8.19}$$

where $\widehat{I} = \int_0^\infty I(a)da$ is the total prevalence in the population, and the time dependence of the variables is implicit. The boundary conditions are $S(0) = \mu$, $I(0) = 0$ at birth, and $S(A_v+) = (1-p)S(A_v-)$, $I(A_v+) = I(A_v-)$ such that there is an instantaneous reduction in susceptibles at age A_v. If we now look for the equilibrium solutions we find that:

$$S^*(a) = \mu \begin{cases} \exp(-(\beta\widehat{I}^* + \mu)a) & \text{for } a < A_v \\ (1-p)\exp(-(\beta\widehat{I}^* + \mu)a) & \text{for } a > A_v \end{cases} \tag{8.20}$$

and:

$$\frac{d\widehat{I}}{dt} = \beta \int_0^\infty S(a)da\,\widehat{I} - \gamma\widehat{I} - \mu\widehat{I} \tag{8.21}$$

$$\Rightarrow \int_0^\infty S(a)da = \frac{\gamma+\mu}{\beta}$$

$$\Rightarrow \frac{1 - p\exp(-[\beta\widehat{I}^* + \mu]A_v)}{\beta\widehat{I}^* + \mu} = \frac{\gamma+\mu}{\beta\mu}. \tag{8.22}$$

It should be obvious from biological principles, if not from equation (8.22), that prevalence, $\widehat{I}^*$, is minimized when $A_v = 0$ and individuals are vaccinated at birth. In such situations protection is offered for the greatest time span possible, reducing the risk of infection to a minimum. When A_v is nonzero, the equilibrium prevalence is more complex to calculate and must be solved numerically (Figure 8.5). For some infections, such as measles, newborns are afforded protection from maternally derived antibodies, as a result of which any effective vaccination must take place after this period of immunity has lapsed. Thus, current MMR (measles, mumps, and rubella) vaccination schedules in most developed nations take place at 12–15 months. This consideration does, however, raise a difficult problem in the developing world where the mean age at infection tends to be very young, leaving a very small window during which infants can be successfully vaccinated before experiencing substantial exposure to infection (McLean and Anderson 1988a,b).

8.1.6.1. Application: Rubella Vaccination

For some diseases, rubella in humans being a prime example, the number of cases within the population as a whole is largely irrelevant; instead, public health policies are concerned with minimizing the number of cases in the most vulnerable classes of the population. Generally, rubella is a benign infection with mild flu-like symptoms—a healthy person typically recovers from infection and may not even realize they have been sick. However, if caught while pregnant the infection can have severe consequences. Infection in the

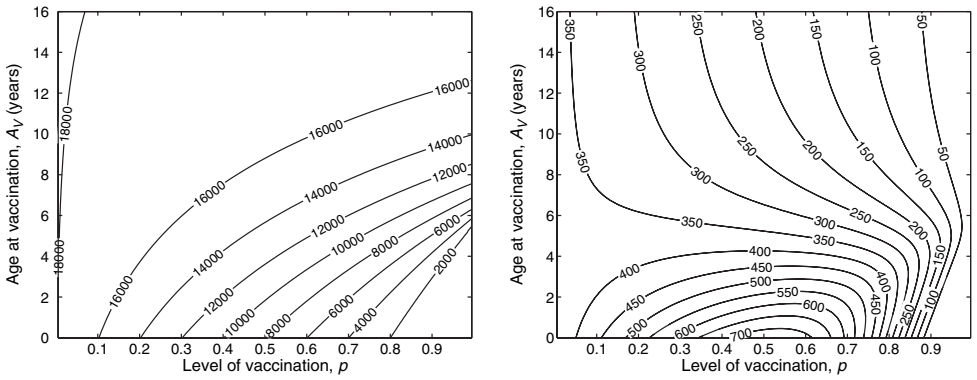

Figure 8.5. The left-hand graph shows the total number of annual cases, $365\gamma\widehat{I}^*$, (in a population of one million), which is determined by solving the age-structured vaccination equation (8.22). Clearly, large amounts of early vaccination are necessary to reduce the prevalence. The right-hand figure shows the number of annual cases of rubella (again in a population of one million) in woman of child-bearing age, which are found from equation (8.23). ($1/\mu = 70$ years, $R_0 = 10$, $1/\gamma = 10$ days.)

first trimester may result in miscarriage, stillbirth, or premature birth. Indeed, one out of four babies infected during the first trimester is born with Congenital Rubella Syndrome, which may result in a multitude of birth defects including mental retardation, cataracts, deafness, cardiac complications, or bone lesions (Behrman and Kliegman 1998). From a public health perspective, we are interested in vaccination strategies that minimize C^*, the equilibrium number of cases in child-bearing women:

$$C^* = \int_0^\infty \beta S(a)\widehat{I}^* P(a)da,$$

where $P(a)$ is the probability that an individual of age a is a pregnant woman.

We can simplify the calculation still further by minimizing the number of cases in women of child-bearing age (say between 16 and 40):

$$C^* = \frac{1}{2}\beta\widehat{I}^* \int_{16}^{40} S(a)da, \tag{8.23}$$

where the $\frac{1}{2}$ is due to the fact that women comprise approximately half of the total population size. Again this value has no explicit expression, but Figure 8.5 shows how the number of cases in the at-risk age group changes as the timing and level of vaccination varies.

Three distinct results emerge. When vaccinating before age 5, intermediate levels of vaccination can increase the number of problematical cases. For most levels of vaccination, it is always better to vaccinate late rather than early. However, for the very highest levels of vaccination (greater than 80%), early immunization more readily limits the impact of the disease.

When the severity of an infection is age-dependent, the interplay between the level of vaccination and the average age of infection can lead to counter-intuitive results where, although moderate amounts of vaccination reduce prevalence they can lead to an increase in disease.

Although such models provide an important understanding of the implications of vaccination when there is a strong age-dependence on the severity of infection, several additional elements would need to be considered if this were to be used for planning public health policy. In particular, the model used above assumes random mixing between age groups, however as was shown in Chapter 3, the differential and assortative mixing between age groups can have a significant impact on the age-structured susceptibility profile, $S(a)$. Additionally, immunization against rubella usually involves a booster vaccine, hence models of the type used in Section 8.1.4 become necessary. Finally, there is the question of targeting the vaccine by gender. Again, this is a complex trade-off; vaccinating girls only makes the best use of a limited vaccine supply but vaccinating both boys and girls has the greatest potential to achieve herd immunity.

8.1.7. Targeted Vaccination

There are many ways in which vaccination, and control in general, can be targeted. The above example showed how targeting of particular age classes may be an effective and efficient control strategy. Other methods are generally based upon protecting those elements of the population that are most at risk. We deal with three specific examples: (1) prophylactic vaccination of individuals based upon their at-risk status, (2) vaccination of individuals identified by contact tracing from sources of infection, and (3) ring vaccination around infectious sources, which has been advocated as a means of controlling livestock diseases.

Consider a population that can be decomposed into two classes, high-risk and low-risk individuals; following the work in Chapter 3, we can model these two classes:

This is online program 8.4

$$\frac{dS_H}{dt} = \mu_H - (\beta_{HH} I_H + \beta_{HL} I_L) S_H - \mu S_H,$$

$$\frac{dI_H}{dt} = (\beta_{HH} I_H + \beta_{HL} I_L) S_H - \gamma I_H - \mu I_H,$$

where subscripts denote the high- and low-risk groups, and a similar equation exists for the susceptibles and infecteds in the low-risk group. (Although the risk-structured models of Chapter 3 were focused toward infections with SIS dynamics, here we assume SIR dynamics but note that both models have the same R_0 and invasion criteria.) For most plausible mixing matrices, $\boldsymbol{\beta}$, we generally find that if the risk structure is ignored, then the estimated value of R_0 is too low, and consequently we underestimate the level of control needed. Once the true value of R_0 is found, either by creating the correct model or more likely by analysis of case reports, then we can again determine a critical level of vaccination that protects the population. Quite surprisingly, if we simply vaccinate at random, then we retain the familiar threshold for the proportion of the population that must be immunized:

$$p_c = 1 - \frac{1}{R_0}.$$

In general, however, we can improve on this threshold. Mathematically, we need to find a level of vaccination for each class, p_H and p_L, such that the effective reproductive ratio, R, is one and the amount of vaccine administered is minimized. (This framework can be generalized to multiple risk groups although the calculations become increasingly difficult.) Unfortunately, an analytical approach to this problem is complex and does not produce any additional understanding. Instead, a numerical approach is required and

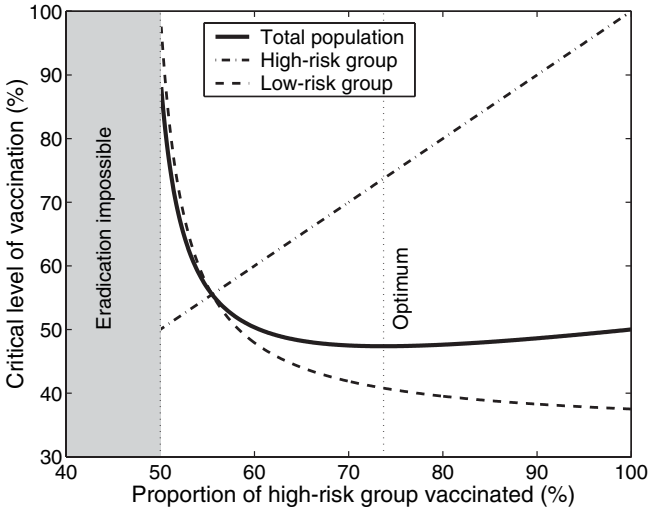

Figure 8.6. The critical level of vaccination needed for eradication, as a percentage of the entire population, for a range of coverage in the high-risk group. In this example, the transmission matrix is $\boldsymbol{\beta} = \begin{pmatrix} 1 & 0.1 \\ 0.1 & 0.2 \end{pmatrix}$ per day, with the proportion of the population in the high-risk and low-risk groups being $N_H = 0.2$ and $N_L = 0.8$, respectively. We take $1/\gamma = 10$ days. For each level of vaccination within the high-risk group, we have searched for the corresponding level of vaccination in the low-risk group that sets the effective reproductive ratio, R, equal to one.

although this cannot produce any rigorous results, it can provide general insights. The most notable is that we can often do much better than the random vaccination threshold when we focus more of our vaccination on the high-risk group. The differences with the random vaccination scenario are most pronounced when a small high-risk group dominates the invasive dynamics. Additionally, although focusing too much vaccination effort on the high-risk group is suboptimal, the penalties are small in comparison to focusing too little effort on this group. Figure 8.6 shows the optimal distribution of vaccine for a given transmission matrix (see Section 3.1.14). For this disease and population structure it is impossible to eradicate the infection unless 50% of the high-risk group are vaccinated. The optimal vaccination policy is to target around 75% of the high-risk group and only 40% of the low-risk group; this bias reflects the relative importance of the two groups in the transmission of infection.

For a general assortative transmission matrix, it is usually better to target vaccination toward the higher-risk groups. Biasing control too much toward high-risk individuals is generally less problematic than biasing control toward low-risk individuals.

Two extreme mixing scenarios are worth further mention, because they bound the standard vaccination approaches. First, consider an infection where the mixing is at random, but proportional to the risk of each class (see the random partnership model, Chapter 3, Section 3.1.1.6). In particular we require the matrix, $\boldsymbol{\beta}$, to be the product of

an exposure (or susceptibility) vector, σ, and transmission vector, τ:

$$\beta_{XY} = \sigma_X \tau_Y$$

and that greater exposure is associated with greater transmission potential ($\sigma_X > \sigma_Y \Rightarrow \tau_X > \tau_Y$). In essence, we simply need that the higher-risk groups are both more at risk of catching the infection and, once infected, have a greater chance of spreading the disease. This is often the case with sexually transmitted infections where both quantities are proportional to the number of partners; however, it may also hold for airborne infections where transmission and susceptibility could scale with the number of social contacts or the immune status of an individual. In such circumstances, vaccine should initially be exclusively targeted at the high-risk group and only once this group is completely immunized should attention switch to the rest of the population. The intuition behind this optimal policy is as follows: Suppose that at any point in the vaccination campaign we have an extra dose that can be administered; it is always better to vaccinate a high-risk individual because, irrespective of the state of the population, they are both most at risk and have the greatest chance of spreading infection—thus immunization of this individual has the greatest effect.

If individuals interact at random but proportional to the risk of each class, then the optimal strategy is to concentrate all vaccination efforts toward the highest-risk individuals.

An alternative transmission matrix is formed when the mixing is completely assortative, so that transmission occurs only within a class and there is no transmission between classes.

$$\beta_{XY} = \begin{cases} \beta_{XX} \geq 0 & \text{if } X = Y \\ 0 & \text{otherwise.} \end{cases}$$

In this case, it is clear that the highest-risk class should be vaccinated first to the point where infection will be eradicated $p_X = 1 - \frac{\gamma}{\beta_{XX}}$, before vaccinating lower-risk groups. This provides the most rapid decrease in R_0 and also a marginally faster reduction in the number of cases.

When mixing is completely assortative it is optimal to vaccinate each class at its eradication threshold.

These two extreme cases provide an understanding of the general rules for targeting vaccination between risk groups—as mixing changes from random to more assortative, the degree of targeting decreases. However, even for completely assortative mixing the vaccine is still targeted due to the higher eradication threshold in the higher-risk groups. Both of these optimally targeted strategies perform significantly better than random vaccination.

8.2. CONTACT TRACING AND ISOLATION

Isolation or quarantining of individuals provides one of the oldest, yet most effective, means of disease control. Although vaccination has to be targeted toward the large pool of susceptible individuals, isolation is focused toward those individuals who are infected—preventing them from further contact and subsequent transmission. There are also substantial microbiological challenges to the successful use of vaccines, especially

when faced with emerging diseases. Vaccination requires that the infectious agent is quickly identified and a safe vaccine is produced and administered. As was seen with the SARS epidemic of 2003, these steps may take a frustratingly long period. In contrast, isolation is effective against any infectious disease even when the etiology is unknown. Finally, whereas there is often a delay between vaccination and immunity, isolation works instantaneously. Therefore, in the majority of outbreak scenarios, the rapid isolation of infected individuals (or those suspected of being infected) is a primary means of control.

The main disadvantage of isolation is that it can be difficult to rapidly identify infectious individuals, especially when symptoms are ambiguous or only emerge sometime after the individual becomes infectious (i.e., when the incubation period is much longer than the latent period). In such cases, contact tracing becomes vital. Contact tracing attempts to identify new cases by tracing all the potential transmission contacts of known infected individuals. Although this is a complex and labor-intensive process, it may be very effective if infectious individuals are rare within the general population (Eames and Keeling 2003).

8.2.1. Simple Isolation

Quarantine can be applied in many ways, but always involves isolating individuals. At the most simple level, infected individuals are quarantined as soon as they are diagnosed. Thus, whereas vaccination acts on susceptible individuals preventing them from becoming infected, quarantine acts by removing infectious individuals from the population, dramatically reducing their risk of transmission. This can be simply modeled by an effective decrease in the infectious period (or an increase in the recovery rate), adding a quarantine class Q to the standard SIR approach:

$$\begin{aligned}
\frac{dS}{dt} &= \mu - \beta SI - \mu S,\\
\frac{dI}{dt} &= \beta SI - \gamma I - d_I I - \mu I,\\
\frac{dR}{dt} &= \gamma I + \tau Q - \mu R,\\
\frac{dQ}{dt} &= d_I I - \tau Q,
\end{aligned} \tag{8.24}$$

where d_I is the rate at which infectious individuals are detected and "removed" to quarantine in addition to the normal recovery rate, and $1/\tau$ is the average time spent in isolation. We assume that individuals leave the quarantine class, Q, only after they have recovered. This leads to a reproductive ratio of

$$R_Q = \frac{\beta}{\gamma + d_I + \mu},$$

so the critical isolation threshold that ensures $R_Q = 1$ is $d_I^* = \beta - \gamma - \mu$.

Contact tracing and isolation are powerful control methods that can be applied to any disease without needing any detailed knowledge of the infection.

Simple isolation of symptomatic individuals acts to reduce the effective length of the infectious period.

The above calculation assumes that the rates of transmission, recovery, and quarantining are independent of the time since infection. A more realistic formulation takes into account the temporally varying rates that are observed. Let us assume that $\beta(T)$ is the transmission rate and $s(T)$ is the probability that symptoms have been observed at time T since infection. Without quarantine, the basic reproductive ratio can be calculated as the infectivity over time:

$$R_0 = \int_0^\infty \beta(T) \exp(-\mu T)\, dT.$$

When quarantine is applied as soon as symptoms are detected, this reduces to:

$$\int_0^\infty \beta(T) \exp(-\mu T)(1 - s(T))\, dT.$$

Hence, even when quarantining as fast as possible, if symptoms are displayed only late in the infectious period (the incubation period is much longer than the latent period), it may be impossible to control an infection by this method alone (Fraser et al. 2004).

We now return to equation (8.24) and consider the effects of logistical constraints on the isolation facility (Cooper et al. 2004). In practice, an isolation facility has a maximum capacity, Q_c, that it can accommodate; for example, Cooper et al. (2004) consider an isolation ward in a hospital in the context of an outbreak of Methicillin Resistant Staphylicoccus Aureus (MRSA), although similar considerations could apply locally or nationally for outbreaks of smallpox, SARS, or pandemic influenza. When the isolation facility is operating below capacity ($Q < Q_c$ or $d_I I < \tau Q_c$), then the dynamics are governed by equation (8.24). However, if infection exceeds capacity ($Q = Q_c$ and $d_I I > \tau Q_c$; the isolation facility is full and there is an excess of infection), newly detected infections can enter isolation only when someone leaves, leading to:

$$\begin{aligned}
\frac{dS}{dt} &= \mu - \beta SI - \mu S, \\
\frac{dI}{dt} &= \beta SI - \gamma I - \tau Q_c - \mu I, \\
\frac{dR}{dt} &= \gamma I + \tau Q_c - \mu R, \\
\frac{dQ}{dt} &= \tau Q_c - \tau Q_c,
\end{aligned} \tag{8.25}$$

in which case the reproductive ratio depends on the current number of cases and is:

$$R_{Q_c} = \frac{\beta}{\gamma + \tau Q_c / I + \mu} > R_Q.$$

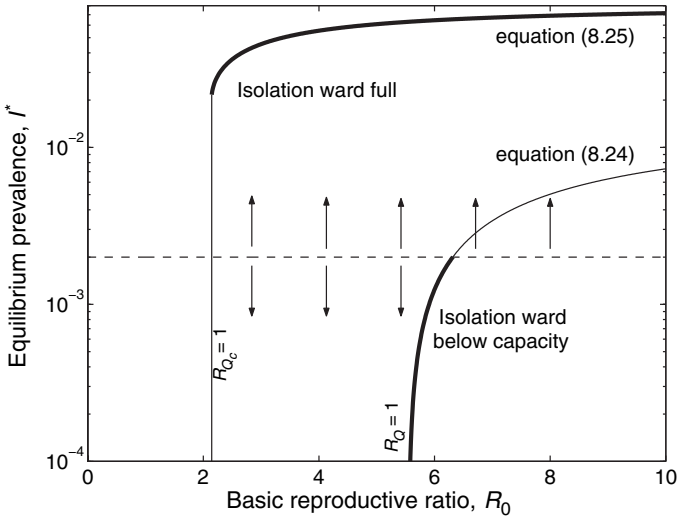

Figure 8.7. The equilibrium behavior of equations (8.24) and (8.25) as the unconstrained basic reproductive ratio $R_0 = \frac{\beta}{\gamma+\mu}$ varies. The dynamics are parameterized to reflect hospital-acquired infections, so that μ measures the rate at which individuals enter and leave the hospital. ($\mu = 0.01$ per day, $d_I = 0.5$ per day, $\gamma = 0.1$ per day, $\tau = 0.1$ per day, $Q_c = 0.01$ measured as a proportion of the hospital population size). Thick lines represent where solutions are stable; the dashed line $d_I I = \tau Q_c$ marks when the isolation ward becomes full and therefore is the boundary between attraction to the two solutions.

Given that there are now two plausible equations, (8.24) and (8.25), two equilibria are now possible (Figure 8.7): one when the isolation ward is below capacity

$$I_Q^* = \mu(R_Q - 1)/\beta,$$

and one when there is an excess of infection

$$\beta(\gamma+\mu){I_{Q_c}^*}^2 + (\beta\tau Q_c + \mu(\gamma+\mu-\beta))I_{Q_c}^* - \mu\tau Q_c.$$

We observe that for some intermediate values of $R_0 (= \beta/(\gamma+\mu))$ the two solutions are both stable. This has a number of far-reaching implications. First, once the quarantine limit is reached the prevalence of infection dramatically increases, jumping from the lower stable solution to the higher stable solution. Second, once the quarantine capacity is reached it may be exceedingly difficult to regain spare capacity because the reproductive ratio, R_{Q_c}, may be much higher. Finally, the size of the isolation facility needed is governed by the prevalence predicted by equation (8.25), and not the normal lower level predicted by equation (8.24)—thus isolation facilities may need to far exceed the usual demand if they are not to succumb to catastrophic failure.

Where isolation or quarantining capacity is limited, bistability can occur. For the same parameters, when the isolation facility is full disease prevalence is high; however, when the facility has spare capacity the incidence of infection can be controlled—both of these solutions are stable.

8.2.2. Contact Tracing to Find Infection

Contact tracing, followed by testing and treatment, is a major weapon in the control of sexually transmitted-infections (STIs). In general, when an individual believes that they are showing symptoms of an STI, they visit their doctor, or a GUM (genitourinary medicine) clinic, where they are tested for the appropriate infection(s). If the test is positive, they are treated and asked for a list of recent (last 6–12 months) sexual partners. These sexual partners, therefore, have an increased likelihood of being infected compared to the general population, and are therefore sought to be tested. If these contacts prove to be infected, then treatment and further contact tracing follows; in this way contact tracing is recursive.

We now define a simple model that captures some of the essential elements of contact tracing for STIs that obey the *SIS* paradigm:

$$\begin{aligned} \frac{dS}{dt} &= -\beta SI + \tau_T T, \\ \frac{dI}{dt} &= \beta SI - d_I I - cbT, \\ \frac{dT}{dt} &= d_I I + cbT - \tau_T T, \end{aligned} \tag{8.26}$$

where T is the class of individuals that are being treated and whose contacts are being traced, with $1/\tau_T$ being the average time in the treatment and tracing class. d_I is the rate at which infected individuals seek treatment and therefore plays the role of the recovery rate, c is the rate of contact tracing, and b is the probability that a traced individual is infectious. We are now faced with the difficulty of determining the value of b. Clearly, if the disease is highly infectious such that every contact leads to the transfer of infection, then $b = 1$; however, at the opposite extreme when contacts are no more likely to be infected than the general population, $b = I$. For simplicity, however, we can initially treat cb as a single parameter that defines the effectiveness of the tracing scheme.

Looking at the equilibrium behavior of equation (8.26) we observe that there are two conditions for disease persistence:

$$\tau_T > cb \qquad \text{and} \qquad \beta(\tau_T - cb) > d_I \tau_T.$$

The first of these ensures that contact tracing is not a runaway process and hence places a limit on the probability b; including iterative tracing, the total number of infected individuals that are traced as a result of an initial detection is $n_T = cb/(\tau_T - cb)$. The second criterion ensures that the basic reproductive ratio (in the presence of contact tracing) is greater than one. Given that these conditions are satisfied we find that:

$$I^* = \frac{\beta(\tau_T - cb) - d_I \tau_T}{\beta(d_I + \tau_T - cb)} = \frac{\tau_T}{\beta}\left(\frac{\beta - d_I(1+n_T)}{\tau_T + d_I(1+n_T)}\right),$$

and we can calculate the basic reproductive ratio by once again using the eigenvalue approach (see Chapter 3):

$$R_T = \frac{\beta}{d_I} - \frac{cb}{\tau_T - cb} = \frac{\beta}{d_I} - n_T,$$

which is equal to the uncontrolled R_0 (β/d_I) minus the number of individuals traced per infectious case. Therefore, if we wish to use contact tracing to eradicate infection, we need to insure that the total number of individuals traced as a result of each initial detection (n_T) is greater than the basic reproductive ratio of the uncontrolled system minus one ($n_T > \beta/d_I - 1$).

One problem with the above set of equations is that the parameter b is unknown, and will change during the course of an epidemic. Several methods can be used to tackle this problem: The methodology outlined in Section 8.3 below is ideal if individuals are generally contacted before they become infectious; alternatively, for STIs one can construct a network of sexual partnerships (see Chapter 3, Figure 3.5) and explicitly model the disease spread and tracing through this network; finally, it is possible to estimate b in terms of the number of infected-infected pairs within the network. This pairwise approach was adopted by Eames and Keeling (2003). By considering that tracing occurred at a much faster timescale than infection, they were able to show that in a range of scenarios the threshold for eradication was approximately that the proportion of contacts traced has to be equal to $(1 - 1/R_0)$—this has strong resonances to the above result and the threshold for vaccination. Intuitively, this ensures that at the threshold each infection causes only one new case that is not traced; however, it is somewhat surprising that this result holds true under such a wide range of heterogeneities.

Contact tracing (followed by isolation) can control an infectious disease if the tracing scheme detects at least all but one of the secondary cases caused.

8.3. CASE-STUDY: SMALLPOX, CONTACT TRACING, AND ISOLATION

Contact tracing is essentially a localized process, such that a complete model should account for the social structure of contacts (e.g., Halloran et al. 2002; Ferguson et al. 2003b; Ferguson et al. 2005); however, substantial progress can still be made using conventional differential equation models. Here we shall illustrate the principles involved with modeling the control of infection using contact tracing and isolation, using smallpox as an example disease, although the models are sufficiently general to be applicable in other scenarios. As mentioned earlier, a major contributing factor to the elimination of smallpox was the dynamic strategy of surveillance, containment, and vaccination of susceptibles in the immediate locality of an identified case (Fenner et al. 1988). The relative merits of these various control options versus prophylactic preemptive vaccination has been a major source of debate in the attempt to prepare potential target nations against any deliberate exposure to smallpox (Kaplan et al. 2002; Halloran et al. 2002; Ferguson et al. 2003b). The major problem relates to vaccine safety becase there are side effects and risks associated with the smallpox vaccine. Although most people experience mild reactions to receiving the vaccine, other people experience reactions ranging from serious to life-threatening. Historically, in a population of one million vaccinated individuals, approximately 1,000 people experienced reactions that, although not life-threatening, were serious (Fenner et al. 1988), and between 14 and 52 people experienced potentially life-threatening reactions to the vaccine, with 1 or 2 fatalities.

When faced with a potential reintroduction of smallpox, policy makers need to decide whether to preemptively mass-vaccinate (e.g., attempt to immunize all 296 million U.S. citizens) or try to locally control any possible outbreaks using the options summarized

TABLE 8.1.
Alternative options for managing any smallpox attack.

Policy	*Benefits*	*Drawbacks*
Quarantine and Isolation		
Sequester suspect and confirmed cases	Highly effective at reducing transmission	Requires rapid and high levels of compliance
Movement Restrictions		
Close schools, airports, and other transport	Potentially useful as shown during 2003 SARS epidemic	Very costly and difficult to implement
Ring Vaccination		
Trace and vaccinate contacts of suspected cases	Optimizes vaccine use and any associated complications	Logistically costly, and needs efficient contact tracing
Targeted Vaccination		
Immunize specific groups or neighborhoods	Effective locally; no contact tracing needed	Requires high levels of herd immunity
Mass Vaccination		
Vaccinate entire population under threat	Effective at widespread transmission control	Large numbers need to be rapidly vaccinated; expensive
Prophylactic Vaccination		
Vaccinate before introduction of disease	Useful to protect "first-responders"; Can prevent rapid spread	High long-term cost; numbers vaccinated

in Table 8.1. In this situation, models can provide useful predictions for choosing among competing options under a range of differing scenarios.

We start by considering an urban population of 1.25 million people, equivalent to a moderately sized city. According to standard theory (Figure 8.1) and assuming an R_0 of 5 (Gani and Leach 2001, Eichner and Dietz 2003), approximately 80% of the population (around 1 million individuals) would need to receive the smallpox vaccine in order to prevent an outbreak. [1] As mentioned above, we may expect serious complications in some 14–52 vaccinated people. The question is whether it would be safer to attempt to use surveillance and containment plus ring vaccination in order to manage any introduction, rather than accept the known complications associated with mass vaccination. Much of the decision in this scenario clearly rests on the perceived likelihood of such an introduction, though the following analyses would be of equal applicability when considering the emergence of novel pathogens.

Consider the simple SIR model, ignoring population demography because it is assumed that the time scale of any outbreak is substantially more rapid than births and background mortality. Although we will often be considering the control of an infection introduced into a totally susceptible population, it is worth noting that for smallpox, some of the

[1] In the absence of any precise new information, this argument assumes that any reintroduced smallpox virus is identical to the historically known pathogen. It is well established, however, that at least the former Soviet Union was active in attempting to combine genes of different viruses (notably smallpox and ebola, and smallpox and Venezuelan equine encephalomyelitis; Alibek 1999). Hence, it is plausible that any new strains of smallpox would bear little resemblance to the "speckled monster" seen in previous decades.

population may have residual immunity either due to past infection or earlier vaccination campaigns. To incorporate contact tracing and isolation, we assume that the traditional transmission parameter, β, is formed from the product of the number of contacts per unit time, k, and the probability of transmitting the disease, b. Again we assume that infectious individuals are detected (and isolated) at a rate d_I, and their contacts are sought. We model contact tracing by forcing a fraction q of those who have recently had contact with an infectious individual to be quarantined where they will spend an average $1/\tau_Q$ days. This occurs both for contacts that are not infected (which are quarantined as X_Q) and those who are infected (which are quarantined as Q)—importantly, we assume that these individuals are quarantined before they have a chance to generate any subsequent infection. Because of this latter assumption, contact tracing does not need to be recursive. This framework will subsequently be made more realistic and complex with the addition of delays in reacting to the epidemic and different distributions of latent and infectious periods, but the simple model will allow us to derive some general results. The equations for this model are given by:

This is online program 8.5

$$\frac{dX}{dt} = -\frac{(kbY + qk(1-b)Y)X}{N} + \tau_Q X_Q, \tag{8.27}$$

$$\frac{dX_Q}{dt} = \frac{qk(1-b)XY}{N} - \tau_Q X_Q, \tag{8.28}$$

$$\frac{dY}{dt} = \frac{kbY(1-q)X}{N} - d_I Y - \gamma Y, \tag{8.29}$$

$$\frac{dQ}{dt} = \frac{qkbXY}{N} + d_I Y - \tau_Q Q, \tag{8.30}$$

$$\frac{dZ}{dt} = \gamma Y + \tau_Q Q. \tag{8.31}$$

where k is the contact rate and b is the probability of transmitting infection to a contact. The absence of host births in this system means that in the event of an infective introduction, the unstable disease-free equilibrium $(N, 0, 0, 0, 0)$ will give way to a brief outbreak, which eventually dies out with $(X_\infty, 0, 0, 0, Z_\infty)$ (see Chapter 2). Therefore, although the dynamics of this system may not be of particular interest, one important quantity is the number of undetected infectives, Y, that occur during the course of the epidemic. Effective infection management would keep this quantity small. We can calculate the conditions required for equation (8.29) to remain negative, which gives the intuitively appealing condition

$$\frac{X}{N} < \frac{X_c}{N} = \frac{(d_I + \gamma)}{kb(1-q)}. \tag{8.32}$$

Efficient contact tracing of susceptibles who have come into contact with infectives (given by parameter q) and rapid isolation of infectious individuals (d_I) effectively reduce the likelihood of an outbreak for an infection with $R_0 = kb/\gamma$. In Figure 8.8, we demonstrate how this threshold changes as a function of the control strategy (contact tracing probability q and isolation rate d_I (per year)) and the infection's R_0. The figure demonstrates that, as

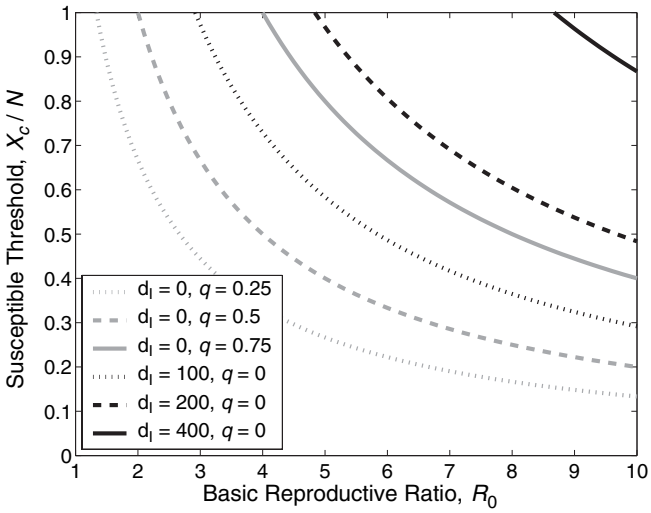

Figure 8.8. The schematic diagram showing the critical threshold fraction of susceptibles necessary for an outbreak as the isolation rate (d_I per year) and quarantine efficiency (q) are varied. Parameter values were $k = 400$ per year and $1/\gamma = 7$ days; b was varied to achieve different R_0 values.

one might expect, $\frac{X_c}{N}$ gets smaller as R_0 increases—an epidemic can occur for a lower level of susceptibles. However, the more useful aspect of the plot is the comparison between the relative effectiveness of contact tracing versus isolating infectives in controlling the infection. We find that rapid detection and quarantining of those infected ($d_I \gg 1$, black lines) is generally a more efficient means of preventing widespread transmission than relying on the successful identification and subsequent isolation of those who recently came into contact with the infection ($q > 0$, gray lines). However, determining the optimal response requires us to estimate the logistical effort associated with these two policies; for example, if contact tracing is much easier than rapid isolation, it may be the preferred strategy despite its weaker impact.

Another important currency for control is the cumulative number of people who contract the infection, especially if infection is associated with serious complications. In Figure 8.9, we plot the cumulative fraction of an initially entirely susceptible population who acquire the infection for various levels of infection management. When q and d_I are small, not surprisingly, a substantial proportion of the population become infected. There is clearly a threshold combination of controls that results in the effective breaking of the chain of transmission. The threshold is derived by studying the necessary conditions for the disease-free equilibrium to become unstable. From equation (8.32), this is given by

$$kb(1-q) > d_I + \gamma.$$

Now let us explore a hypothetical set of scenarios. Consider the introduction of a smallpox-like infection, with highly detectable symptoms for which an efficacious vaccine was available. The vaccine is assumed to be associated with a small chance of serious

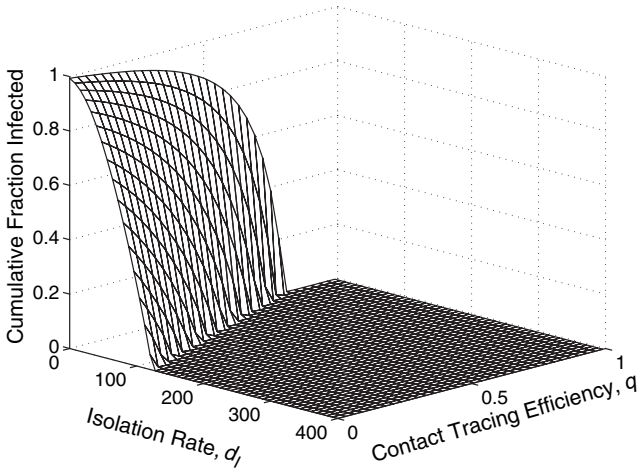

Figure 8.9. The cumulative fraction of the population infected as the isolation rate (d_I) and quarantine efficiency (q) are varied, using equations (8.27) to (8.31). Parameter values were $k = 230$ per year, $1/\gamma = 12$ days, $1/\tau_Q = 21$ days, and $b = 0.65$, such that $R_0 \approx 4.9$.

side effects. Assuming all economic costs and possible logistic obstacles and delays can be overcome, is it "best" to (1) vaccinate a large fraction of the population, (2) attempt to manage any introduction by surveillance and containment, plus additional vaccination? Of course, to some extent the answer depends on what we mean by best. Possible important measures of optimality may include the fewest number of cases, the fewest fatalities, and the shortest duration of outbreak. In order to examine this situation, we use equations (8.27)–(8.31) with the addition of an (asymptomatic and undetectable) exposed class. We assume $R_0 \sim 5$, and that the mean latent and infectious periods are both 12 days (Gani and Leach 2001). Background vaccination levels, p, of 40%, 60%, and 80% are explored by setting $X(0) = N \times (1 - p)$. We assume surveillance and containment to include the daily identification and quarantine for 3 weeks of 30% of infectious cases ($d_I = 120$ per year), along with 50% of susceptible contacts ($q = \frac{1}{2}$). The results of this experiment are presented in Table 8.2.

These findings are informative because they highlight different consequences of alternative courses of action. Clearly, if p_c $(= 1 - 1/R_0)$ fraction of the population are vaccinated, then $\frac{dI}{dt} < 0$ and any introduction will be unsuccessful, with a very brief period of public concern. The downside to such a strategy is that vaccinating 80% of the population will present substantial logistical challenges in addition to the great financial cost. In addition, in this example, of the one million people vaccinated, around 15–50 individuals may experience very serious side effects. On the other hand, in the absence of prophylactic vaccination, a policy of contact tracing and isolation in the event of any smallpox introduction will result in no vaccination-induced complications, only 73 cases, 11 infection-induced deaths, and an outbreak that lasts less than 25 weeks. This is based on quarantining 50% of contacts, as well as the isolation of one-third of all infectious individuals per day—the implementation of both of these measures is likely to be expensive

TABLE 8.2.
Outcomes of alternative control measures when 10 infectious individuals are introduced into an entirely susceptible urban population of size 1.25 million. We assume that half of all contacts are traced ($q = 0.5$), and that isolation takes an average of 3 days ($d_I = 0.33$ per day). The probability of infection-induced mortality is assumed to be 15%.

Control Measure	*Cases*	*Deaths*	*Duration of Epidemic*	*Peak Number of Infectives*	*Number Vaccinated*
Mass Vaccination					
40%	708,303	106,250	52 weeks	112,571	500,000
60%	403,667	60,550	84 weeks	39,692	750,000
80%	< 10	< 1	2–3 weeks	< 10	1,000,000
Contact Tracing	1,082,040	162,306	71 weeks	67,346	0
Isolation	741,334	111,200	56 weeks	18,958	0
Contact Tracing and Isolation	30	4	18 weeks	10	0

and logistically challenging. Table 8.2 shows that isolating known contacts or infectives alone is not very effective, whereas the two in conjunction can drastically control any epidemic. This is because although each control measure in isolation produces a reduction in R_0, the reduction is not sufficient to bring R_0 close to (or below) one and hence a significant epidemic still occurs.

Although such analyses can be illuminating from a general perspective, in order to make quantitative predictions on infection management, we need to take into account a number of important biological details (Ferguson et al. 2003b; Lloyd-Smith et al. 2003; Wearing et al. 2005). First, we note that the incubation period (time taken from infection to exhibit symptoms) exceeds the latent period, so we split infectious individuals into those who are exhibiting symptoms (I_S) and those without symptoms for whom the incubation period has not elapsed (I_A). Second, we incorporate a more realistic distribution into the latent and infectious classes (see Chapter 3). All periods are assumed to be gamma distributed; the exposed period is subdivided into m_E classes and has an average length of $1/\sigma (= 12$ days), the asymptomatic infectious period (I_A) is divided into m_A classes and has an average length $1/\gamma_A (= 3$ days), and the symptomatic infectious period (I_S) is divided into m_S classes and has an average length $1/\gamma_S (= 9$ days).

We again construct the model by considering the fate of each susceptible-infectious contact, which occur at rate kXY/N. The susceptible involved in such a contact can be classified into one of four different states and these are modeled separately: (1) A proportion $(1-q)(1-b)$ are uninfected and never uncovered as part of the contact tracing from the infected contact; these remain in the susceptible class X. (2) A proportion $(1-q)b$ are infected but never uncovered by the tracing; these progress into the first exposed class W_1 and eventually become infectious. (3) A proportion $q(1-b)$ are uninfected but detected as part of the contact tracing scheme; these are isolated in class X_Q and are only released a time τ_Q after the initial contacts when it can be certain they will not develop symptoms. (4) The remaining proportion qb are infected and are assumed to be uncovered by tracing before they become infectious. These are labeled Q; although these individuals pass through exposed and infectious stages these do not need to be modeled as they have no effect on the rest on the population because the individual will be isolated. The system

of equations describing such a model is given by:

$$
\begin{aligned}
\frac{dX}{dt} &= -\frac{(b+q(1-b))kX(t)Y(t)}{N} + \frac{q(1-b)kX(t-\tau_Q)Y(t-\tau_Q)}{N},\\
\frac{dX_Q}{dt} &= \frac{qk(1-b)X(t)Y(t)}{N} - \frac{qk(1-b)X(t-\tau_Q)Y(t-\tau_Q)}{N},\\
\frac{dW_1}{dt} &= \frac{(1-q)bkX(t)Y(t)}{N} - m_E\sigma W_1(t),\\
\frac{dW_i}{dt} &= m_E\sigma W_{i-1}(t) - m_E\sigma W_i(t), \quad i = 2,\ldots,m_E,\\
\frac{dY_{A,1}}{dt} &= m_E\sigma W_m(t) - m_A\gamma_A Y_{A,1}(t),\\
\frac{dY_{A,i}}{dt} &= m_A\gamma_A Y_{A,i-1}(t) - m_A\gamma_A Y_{A,i}(t) \quad i = 2,\ldots,m_A,\\
\frac{dY_{S,1}}{dt} &= m_A\gamma_A Y_{A,n_A}(t) - (m_S\gamma_S + d_I)Y_{S,1}(t),\\
\frac{dY_{S,i}}{dt} &= m_S\gamma_S Y_{S,i-1}(t) - (m_S\gamma_S + d_I)Y_{S,i}(t), \quad i = 2,\ldots,m_S,\\
\frac{dQ}{dt} &= \frac{qbkX(t)Y(t)}{N} + d_I Y_S(t),\\
\frac{dZ}{dt} &= m_S\gamma_S Y_{S,m_S}(t),
\end{aligned}
\tag{8.33}
$$

where, for convenience, $Y = \sum_{i=1}^{m_A} Y_{A,i} + \sum_{i=1}^{m_S} Y_{S,i}$. Note that here R represents those who recover before they could be isolated or quarantined and therefore those who spend their entire infectious period in the population at large. As the epidemic dies out, $Q + R$ will represent the total number of recovered individuals, because Q keeps track of all those infected individuals who are quarantined or isolated, and effectively removed from the infectious population. Note that we do not adjust N in the denominator of the frequency-dependent mixing term to discount those in quarantine when calculating the contact frequency because we want to assume that the level of mixing remains the same following interventions. Finally, if we wished to accurately represent the known epidemiology of smallpox, we would insist that the contact rate k and the transmission probability b are different for the asymptomatic and symptomatic classes, matching the observation that asymptomatics have more contacts but are less infectious ($k_A > k_S$ and $b_A < b_S$) (Eichner and Dietz 2003). However, due to uncertainties in the parameterization of this extra heterogeneity, we will assume uniform parameter values for simplicity.

As shown in Figure 8.10, the precise levels of isolation of infecteds (d_I) and quarantining (q) required to control the outbreak and the predicted level of disease incidence are affected by whether asymptomatic infectious individuals are successfully traced and isolated, or whether this is achieved only for those with pronounced symptoms. Here we are envisaging the situation where contacts are requested for the past 12 days compared to asking for contacts since the infectious person first started to feel ill. It is not surprising that if the

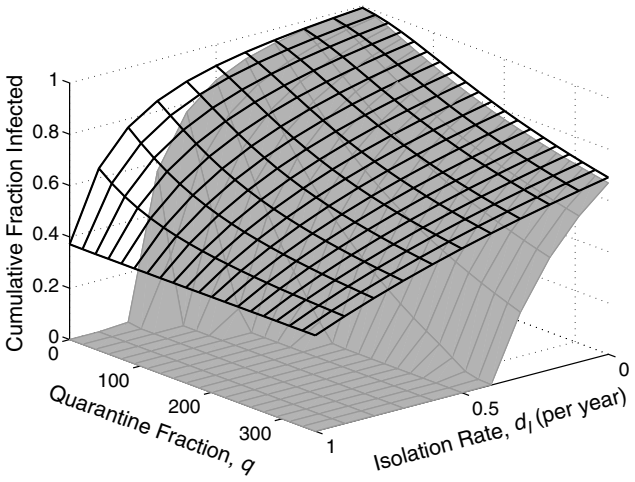

Figure 8.10. The predicted effectiveness of contact tracing and isolation of infectives in a population of 1.25 million susceptibles. The surfaces represent predictions of the model given by equation (8.33) with either contacts with all infected individuals traced and isolated (gray) or only those with pronounced symptoms (black). Although the surface can be calculated from equation (8.33), the black grid requires some modification to the model, separating those in contact with symtomatic and asymtomatic individuals. The figure demonstrates that if the infection is associated with a significant undetectable infectious stage (black grid), effective control is very difficult. (Model parameters $m = 45$, $n_A = 5$, $n_S = 8$, $k = 235$, $b = 0.65$, $1/\sigma = 12$ days, $1/\gamma_A = 3$ days, $1/\gamma_S = 9$ days, $\tau_Q = 20$ days.)

disease is associated with a substantial asymptomatic or undetectable infectious phase, then effective control that relies on the identification of infection is difficult. The figure also demonstrates that quarantining has a greater effect on reducing the cumulative fraction of the population infected than isolation.

Using a slightly more complex infection control model that incorporated a delay between becoming infectious and implementing isolation, Wearing et al. (2005) highlighted an additionally important aspect of such models. (In this model, isolation at rate d_I does not begin until τ_D days after an individual becomes infectious.) They demonstrated that models with exponential waiting times in the infectious period predict more optimistic outcomes of control compared to those with a gamma distribution (see Chapter 3). The explanation for such an observation lies in the process of isolating infectives, which reduces the effective mean infectious period (Wearing et al. 2005). Accounting for the isolation of infecteds at rate D_I after a delay of τ_D days, the average infectious period for the exponentially distributed model ($n_A = n_S = 1$) is

$$\frac{1 - e^{(-\gamma\tau_D)}}{\gamma} + \frac{e^{(-(\gamma+d_I)\tau_D)}}{\gamma + d_I}. \tag{8.34}$$

In contrast, the mean infectious period for a fixed infectious period ($n_A, n_S \to \infty$) is given by

$$\tau_D + \frac{1 - e^{(-d_I(1/\gamma - \tau_D))}}{d_I}. \tag{8.35}$$

From these equations, the isolation of infecteds is predicted to be much more effective when the infectious period is exponentially distributed because it essentially truncates the long tail of the distribution, so that the infectious period of a few individuals is dramatically reduced. This effect is not as pronounced in the gamma-distributed models because there is less variation in the infectious periods. Indeed, as long as the infectious period in the absence of isolation is greater than the delay ($1/\gamma > \tau_D$), then expression (8.34) is less than expression (8.35) for all $d_I > 0$ (Wearing et al. 2005). In the same way, a longer delay in detecting infected individuals has fewer predicted consequences for the exponentially distributed model because during this time many individuals will have naturally left the infectious class. Under the assumption of a gamma-distributed infectious period, most individuals are infectious for a minimum period of time so early detection is more important. Although the predicted difference between the exponential and gamma-distributed models depends on the duration of the infectious period and the fraction of contacts traced (q), it is generally true that models with an exponentially distributed infectious period will give rise to overly optimistic predictions concerning the effectiveness of isolating infectives.

A further important point to notice from comparing Figures 8.9 and 8.10 is that similar levels of infection management are predicted to result in dramatically reduced infection control. Indeed, irrespective of the assumptions made on latent and infectious period distributions in equation (8.33), the rapid removal of symptomatic infectives ($d_I = 365$) and quarantine of 80% of contacts is still predicted to result in almost 20% of the population contracting the infection (Figure 8.10). In contrast, the results in Figure 8.9 suggest that eradication is relatively easy. The primary cause for this substantial and very important difference between the two model results is the introduction of the effective delays in implementing controls. The take-home message from Table 8.2 is that effective isolation and quarantine can successfully contain any introduced infection, whereas the results shown in Figure 8.10 demonstrate that in reality this is very difficult, perhaps even unlikely. This work points toward the need for additional (and possibly targeted) vaccination in order to suppress an outbreak. This topic, along with the spatial consequences of such actions, are discussed in the next section.

8.4. CASE-STUDY: FOOT-AND-MOUTH DISEASE, SPATIAL SPREAD, AND LOCAL CONTROL

One of the best demonstrations of the usefulness of mathematical models was during the high-profile 2001 epidemic of foot-and-mouth disease (FMD) in the United Kingdom. As with the smallpox case study, modeling is useful due to the complex trade-off between culling and control: Too little culling and the disease is not controlled; too much culling and although the disease is eliminated, many more livestock may be lost due to culling. As discussed in Chapters 4 and 7, this infection is made more complex by the presence of more than one host (sheep, cattle, and pigs, though pig farms were largely unscathed in the 2001 outbreak) and the spatial aspect of transmission, combining both localized farm-farm interactions and longer-range transmission due to movements of machinery and personnel. To model the 2001 outbreak, Keeling et al. (2001b) developed a stochastic, spatially explicit farm-based model. This framework contains the inherent assumption that transmission within a farm is rapid, hence it is reasonable to categorize each farm

as susceptible or infected. Once fully parameterized, the model was used to investigate different options for managing the epidemic.

After the first reported case on February 20, 2001, the FMD virus spread rapidly across the country, with over 600 farms infected within the first 5 weeks of the epidemic. To control the outbreak, the UK Ministry of Agriculture, Fisheries and Food (MAFF) instigated a national ban on livestock movement, together with a requirement for all livestock on infected farms (called infected premises, or IPs) to be culled within 24 hours of the infection being reported. In addition, the livestock on at-risk farms (dangerous contacts, DCs, and contiguous premises, CPs) were also to be culled within 48 hours of FMD detection on the associated IP. Conceptually, we can equate control of dangerous contacts with contact tracing, whereas control of contiguous premises is comparable with local measures such as ring culling. Eventually, in October 2001, the epidemic was declared over. More that 2,000 farms had been infected and over 8,000 culled as part of the control. Given the catastrophic economic cost of implementing measures to control the epidemic, as well as its consequences for UK industries (such as farming and tourism), the newly formed Department of Environment, Food and Rural Affairs (DEFRA) was interested in developing protocols for future management strategies. Mathematical models played an important role in the formulation of DEFRA's contingency plan, published in 2004, which now contains the provision for localized vaccination against a future epidemic.

Box 8.1 Individual-Based FMD Model

As described in Chapter 7 (see also Keeling et al. 2001b; Keeling et al. 2003; and Tildesley et al. 2006), the transmission of foot-and-mouth disease can be modeled using a spatial transmission kernel, $K(d)$, which is a function of the distance d between the infecting and susceptible farm. The rate λ_i at which susceptible farm i becomes infected is given by:

$$\lambda_i = Sus_i \sum_{j \in \text{infectious}} Trans_j \, K(d_{ij}),$$

$$Sus_i = \sum_{l \in \text{species}} N_{i,l} \, s_l, \qquad Trans_j = \sum_{l \in \text{species}} N_{j,l} \, t_l$$

where $N_{i,l}$ is the number of livestock of type l on farm i and s_l and t_l are species-specific susceptibility and transmissibility for cattle, sheep, and pigs. The model is iterated forward daily by performing the following two steps:

1. Each susceptible farm is infected with probability $1 - \exp(-\lambda_i)$.
2. The time since infection for each infected farm is increased (by one day) and the status of the farm is updated appropriately. Farms that have been infected for between 0 and 5 days are assumed to be exposed, those infected for more than 5 days are infectious, whereas those infected for 9 days are symptomatic.

In addition to the epidemiological dynamics, a range of culling strategies also need to be modeled. The processes involved are detailed below.

IP Culling

Infected premises (IPs) should have their livestock culled as quickly as possible following detection of the disease, so as to reduce the infectious period by as much as possible. This process is modeled by removing the farm (by setting $N_{i,l} = 0$) τ_{IP} (usually equal to 1) days after the disease is identified; in general, this is between 10 and 15 days after infection.

DC Culling

Dangerous contacts (DCs) are conceptually equivalent to traced contacts; they are farms that are assumed to be at a high risk of infection due to their connections with an identified IP. If farm i is an infected premise, then the probability that farm j is a dangerous contact is

modeled as

$$\begin{cases} 1 - f\exp(-FSus_j Trans_i K(d_{ij})) & \text{if } j \text{ has been infected by } i \\ 1 - \exp(-FSus_j Trans_i K(d_{ij})) & \text{otherwise,} \end{cases}$$

where the parameter F accounts for the number of DCs identified and culled per IP, and the parameter f accounts for local knowledge of potential transmission routes, which increases the accuracy of identifying infected farms. After a delay of τ_{DC} (usually equal to 2) days from when an infected farm is diagnosed, all of the livestock on the associated DC that can be identified are culled. In general, an average of one or two DCs are usually identified per infected farm.

CP Culling

Contiguous premise (CP) culling was initiated as an alternative strategy to a fixed-size ring cull, targeted toward farms that share a common boundary. Although in practice CPs are identified using detailed maps of farm boundaries, this information is not available electronically and so some approximate criteria needs to be defined. We construct CPs by assuming that farms tessellate across the landscape, such that the boundary between two farms is given by a perpendicular line halfway between their coordinates (dashed line on the figure below).

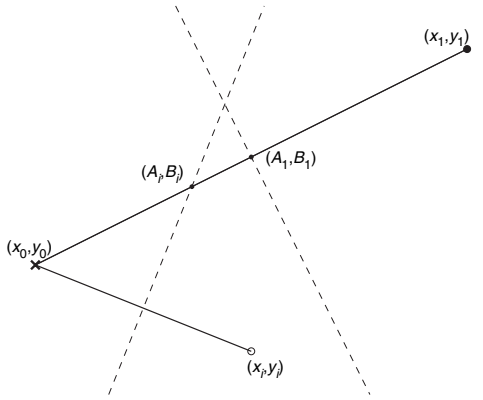

Graphical representation of the methodology for determining contiguous premises in terms of the positions of potential boundaries (shown as dashed lines).

As a simple approximation, farm 1 at position (x_1, y_1) is considered to be contiguous to farm 0 at position (x_0, y_0) if their boundary is closer to farm 0 than any other boundary:

$$\frac{\left(\frac{(y_i - y_0)^2 + (x_i - x_0)^2}{(y_i - y_0)}\right)}{(x_1 - x_0)\left(\frac{(y_1 - y_0)}{(x_1 - x_0)} + \frac{(x_i - x_0)}{(y_i - y_0)}\right)} > 1 \quad \forall i.$$

In the full simulation models (Keeling et al. 2001b; Keeling et al. 2003; and Tildesley et al. 2006) account was also taken of the relative areas of the farms, which biased the position of the boundary and limited the potential for very distant farms to share a boundary.

CP culling then takes place τ_{CP} (usually equal to 2) days after the infected farm is identified by culling all the animals on a proportion p_{CP} of all the contiguous premises of the IP.

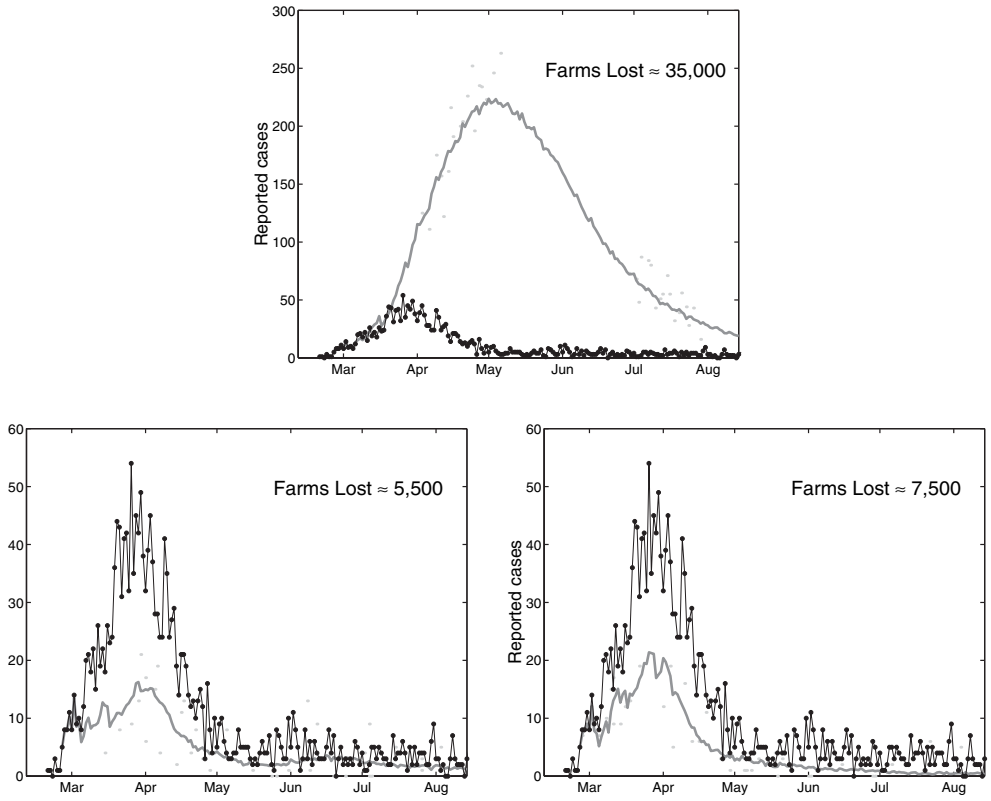

Figure 8.11. The figure demonstrates the effects of varying the culling procedure on the epidemic curve (from Keeling et al. 2001b). Black dots denote actual reported cases, and pale gray dots are the results of 50 simulations, with the thick gray line giving the average of those simulations. Data is shown only until the middle of August for greater clarity. In the top graph, only the IP cull is performed with the delay between reporting and culling following the pattern observed in 2001. The culls in the bottom-left graph follow the observed level, but the delays from reporting to slaughter of the animals on the IP and from reporting to culling of animals on DCs and CPs are assumed to be prompt (24 and 48 hours, respectively) from the beginning of the simulation. In the bottom-right graph, the delays now follow the observed pattern, but the levels of CP and DC culls are constant throughout the simulation and mimic the high levels achieved in the latter part of the 2001 epidemic. The inset values on each graph give the average number of farms losing their livestock either due to infection or control measures.

Modeling demonstrated that culling IPs, CPs, and DCs, as performed in 2001, was effective at controlling the epidemic with minimal consequences (Figure 8.11). Had the cull been restricted to IPs only—just targeting identified sources of infection—then a total of over 35,000 farms are predicted to have been infected. On the other hand, if the 24–48 hour time scale from reporting to cull had been imposed from the very beginning (bottom-left graph), or the higher culling levels achieved later on in the epidemic had been exercised earlier (bottom-right graph), then the total number of farms affected and

animals slaughtered could have been substantially reduced. This echoes a general tenet in epidemiology, that it is often a good idea to apply control measures promptly and intensively; however, as shown in Chapter 7, Figure 7.17, which examines ring culling for the same model, if the control measures are too intensive, their consequences can be worse than the epidemic itself.

Planning for any future FMD outbreak has inevitably involved detailed *scenario modeling* involving a range of different strategies. Vaccination remains an important tool in the control of any disease, and could potentially be used against FMD in the future. Vaccination was not implemented during 2001, due to logistical constraints and the modeling predictions that vaccination late in the epidemic would be ineffective (Keeling et al. 2001b; Keeling et al. 2003). The most important aspect of modeling the effects of vaccination is the recognition of three key biological properties of FMD vaccines. First, these vaccines do not provide complete protection, with typical efficacies in the 90–95% range (Barnett and Carabin 2002). It is generally assumed in these models that 90% of vaccinated animals are fully protected, whereas the remaining 10% are fully susceptible, although this is an approximation to the complex reality of immunization. This means that, although all the animals on a farm may be vaccinated, some of the animals may remain susceptible so that the farm can still become infected and act as a source of further cases. Second, as with other vaccines, FMD vaccines do not provide immediate protection; the high potency vaccines may protect within 3–4 days, whereas standard vaccines take considerably longer, around 10 days (Woolhouse 2003). Third, vaccination has no or limited effect on animals that are already infected. Finally, vaccination provides only short-duration protection and repeated vaccination may be required every 6 or 12 months. These traits clearly need to be taken into account when considering future vaccination campaigns.

One option for preventing future epidemics is to maintain a high level of herd immunity to FMD within the UK livestock population, similar to the vaccination policies against childhood diseases (see Section 8.1.1), although requiring repeated vaccination. Such prophylactic vaccination, together with the culling of infected and at-risk Dangerous Contact (DC) farms, has a strong effect on the final epidemic size (Figure 8.12). In general, the vaccination of cattle in 25,000 randomly chosen farms reduces the size of the epidemic to levels similar to those achieved by stringent and expensive IP, DC, and CP culling procedures. If over 80,000 farms can be protected from infection (which requires the vaccination of most cattle in the United Kingdom), then any introduction of the FMD virus is very unlikely to result in further spread. The precise effect of vaccination is determined in part by the strategy for selecting which farms to vaccinate; the preferential immunization of large cattle farms, which are generally at greater risk, is significantly more effective than simple random vaccination. Again, this echoes results from Chapter 3, where control should be targeted toward high-risk individuals—in this case, large cattle farms that have a high susceptibility and transmissibility.

The right-hand graph of Figure 8.12 examines the results of a range of other prophylactic vaccination options. First, we consider vaccination of sheep and pigs as well as cattle. Although in practice this would be more difficult to achieve, it is heuristically useful to explore in terms of the impact of population-level immunity. Not surprisingly, the vaccination of all three species (dashed lines) gives rise to smaller epidemics than vaccinating cattle alone. However, if we consider the effective control achieved as a function of the total numbers of animals vaccinated, then concentrating on cattle alone is much more efficient. This graph also stresses the need for maintaining DC culling (comparing black and gray curves). If DC culling were relaxed (gray curves), because

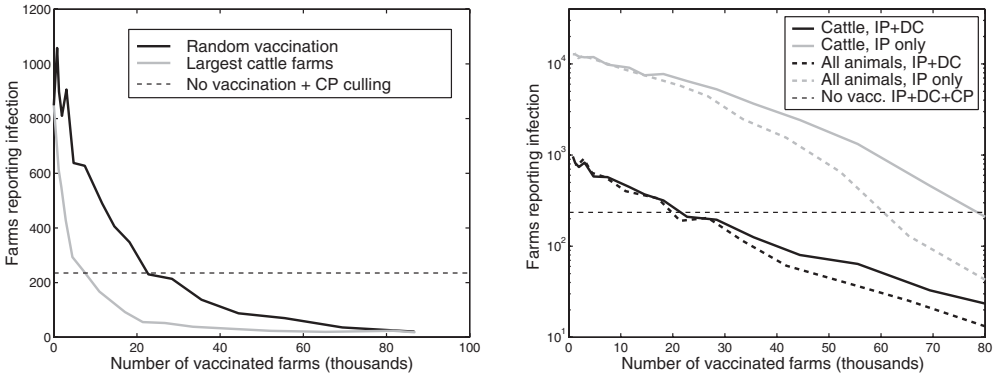

Figure 8.12. The fate of an FMD introduction into five randomly chosen farms in Great Britain after prophylactic vaccination, from Keeling et al. 2003. IP and DC culls (averaging one DC per IP) were used to control the epidemics, and movement restrictions were enforced two weeks after the arrival of the disease. CP culling was not performed due to the strong opposition to this strategy in 2001; however, a comparison is made to the case where 70% CP culling is used instead of vaccination (horizontal dashed line). Results are the average of 500 simulations; in many of which the epidemic fails to take off, we generally assume that only cattle are vaccinated and the efficacy is 90%. The graphs show the effect of changing the number of farms that are vaccinated before the epidemic begins. The left-hand graph shows the average number of farms reporting infection for two different vaccination approaches. The right-hand graph compares the effects of vaccinating just cattle (solid lines) and all animals (dashed lines), and the effects of IP and DC culling (black lines) with IP-only culling (gray lines)—vaccination is at random.

it was felt that vaccination gave sufficient protection, then the expected number of cases increases tenfold compared to a combined DC-culling and vaccination strategy.

As mentioned in Table 8.1, one of the drawbacks of prophylactic vaccination is the need for long-term maintenance of substantial herd immunity, the cumulative cost of which is very large. Instead, reactive vaccination—the immunization of livestock after an outbreak has been detected—may represent a more appealing option. Tildesley et al. (2006) have investigated the possibility of using ring vaccination to control any future epidemic. It is assumed that ring vaccination will be a successful control measure because it is targeted at farms surrounding an infected premise. These farms are known to be at greater risk of infection due to the localized transmission of foot-and-mouth disease (see Section 7.5.2). However, if the farm is already infected, vaccination is assumed to have no effect; therefore, very localized vaccination may often be infective. In agreement with known vaccine behavior (Barnett and Carabin 2002) and adopted UK policy (DEFRA 2004), we assume that a combination of IP culling, DC culling, and ring vaccination are applied and that cattle on farms within a ring surrounding each reported premise are identified for vaccination 2 days after reporting. Due to logistic constraints (in terms of the number of vaccination teams available), only a limited number of cattle can be vaccinated on each day—these are prioritized in the order in which the central infected farm is identified. This logistic constraint generates a trade-off within the model: If the vaccinated ring is too small, too few animals will be protected; in contrast, if the vaccination ring is too large, the constraint on the number of cattle that can be vaccinated per day means that considerable delays may develop.

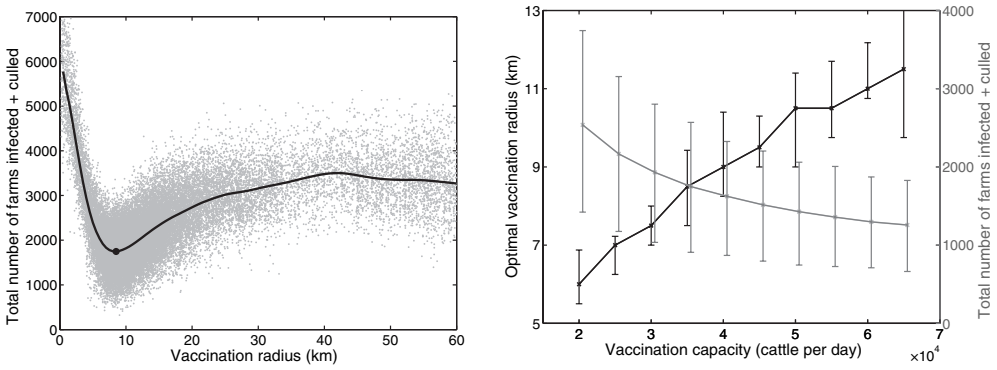

Figure 8.13. Results from detailed stochastic spatial simulations of foot-and-mouth disease in the United Kingdom, taking into account farm heterogeneity and animal composition; parameters are derived by fitting to the behavior of the 2001 epidemic, from Tildesley et al. (2006). Control is a mixture of IP culling within 24 hours of detection, DC culling 24 hours later, and ring vaccination. The left-hand graph shows the total loss of farms (due to either infectious or culling) for various ring sizes when there is the capacity to vaccine 35,000 cattle per day; the gray dots are the results of individual simulations, the black curve is a smoothed fit to the mean, and the large black dot gives the position of the optimal radius. In the right-hand graph, this concept is extended and the optimal ring size and total loss of farms is shown as the vaccination capacity varies. Throughout it is assumed that the vaccine has an efficacy of 90% and that there is a delay of 4 days between vaccination and protection.

The left-hand graph of Figure 8.13 shows how the number of farms lost (either due to infection or DC culling) varies with the size of the vaccination ring. Clearly there exists an optimal vaccination radius that maximizes the number of cattle vaccinated per day but minimizes the delay. This optimal vaccination strategy (combined with IP and DC culling) leads to the loss of far fewer farms than a more intensive cull-based control in which IPs, DCs, and CPs are culled—thus demonstrating the advantages of well-targeted vaccination. The right-hand graph demonstrates how the optimal vaccination radius (gray line) and the number of farms lost (black line) is affected by the vaccination capacity. As expected, when more cattle can be vaccinated per day, the optimal radius can increase and hence the total number of farms lost decreases—however, there is no simple relationship between vaccination capacity and optimal ring size, illustrating the need for complex simulation models that can account for the spatial structure and heterogeneities present in the UK farming landscape.

8.5. CASE-STUDY: SWINE FEVER VIRUS, SEASONAL DYNAMICS, AND PULSED CONTROL

Another arena where mathematical models can be usefully employed is the examination of emerging infectious diseases, such as AIDS, severe acute respiratory syndrome (SARS), or the new influenza A viruses (Morens et al. 2004). These emerging infectious diseases (EIDs) are especially interesting and important because the threat they pose is not confined to humans, with documented examples in animal (Daszak et al. 2000) and plant (Anderson

et al. 2004) species. It is now apparent that a substantial proportion of emerging infectious diseases are due to novel pathogens that have managed to cross species boundaries (Antia et al. 2003; Woolhouse et al. 2005). Typical examples include the simian origin of HIV (Hahn et al. 2000), and the identification of viruses related to the SARS coronavirus in small asiatic mammals (Guan et al. 2003). Consequently, the origins of marburg and ebola viruses are currently sought in African wildlife populations (Monath 1999).

Cross-species pathogen transmission also seems to be a common phenomenon between free-living wild animal populations and their domestic counterparts (Daszak et al. 2000), with pathogen transmission generally facilitated by the genetic relatedness of the two host species. An additional aspect of these systems is that many of the free-living wild animal populations that harbor infectious diseases of potential threat are often hunted for recreation and/or population regulation. Here, we follow Choisy and Rohani (2006) and examine a simple general model that accounts for the dynamics of a directly transmitted disease in a harvested/hunted host population.

The general framework we introduce here is intended to mimic the dynamics of a viral or bacterial disease in a harvested population of wild ungulates, in a temperate region. The underlying motivation behind this model is to assess the role of culling wild boar to reduce the transmission of classical swine fever (CSF) to domestic livestock. We consider a naturally regulated host population that experiences infection by a directly transmitted microparasitic disease conferring permanent immunity to those recovered. The general structure of the model is as follows:

$$\frac{dX}{dt} = \varphi(t)N(t)\nu(N) - [\mu_X(N) + \psi(t)q_X H_X + \lambda(t)]X(t), \tag{8.36}$$

$$\frac{dW}{dt} = \lambda(t)X(t) - [\mu_W(N) + \psi(t)q_W H_W + \sigma]W(t), \tag{8.37}$$

$$\frac{dY}{dt} = \sigma W(t) - [\mu_Y(N) + \psi(t)q_Y H_Y + \gamma + m]Y(t), \tag{8.38}$$

$$\frac{dZ}{dt} = \gamma Y(t) - [\mu_Z(N) + \psi(t)q_Z H_Z]Z(t), \tag{8.39}$$

where, as usual, the variables X, W, Y, and Z represent the numbers of susceptible, exposed, infectious, and recovered animals, respectively. We stress that the total population size $N(t)$ $(= X + W + Y + Z)$ is not necessarily constant. The term $\nu(N)$ is the per capita density dependent birth rate, and $\mu_i(N)$ is the per capita density-dependent natural death rate in compartment i $(i \in \{X, W, Y, Z\})$. Parameters q_i $(0 \le q_i \le 1)$ and H_i are, respectively, the catchability and the harvest effort in compartment i, reflecting the fact that infected animals may behave differently (Kot 2001). Susceptible individuals get infected at a rate given by the force of infection $\lambda(t) = \beta \frac{Y(t)}{N(t)}$, where β reflects the transmission rate and we are assuming frequency-dependent transmission. Although wildlife diseases are generally modeled using density-dependent transmission, the social structure within the wild boar population means that frequency-dependent transmission is a better assumption, although the truth is likely to lie between the two. We assume that the mean duration of the exposed and infectious periods are given by $1/\sigma$ and $1/\gamma$, respectively—taking the simplest assumption of constant rates rather than explicit distributions. Finally, the disease can induce additional mortality on the infectious individuals, at a rate m.

In most large herbivore species, it is well documented that births and deaths are density dependent (Gaillard et al. 2000). For simplicity, we assume that these two (per capita) rates

are linearly related to population density such that

$$\nu(N) = b - BN(t-\tau), \tag{8.40}$$

$$\mu_i(N) = d_i + D_i N(t), \tag{8.41}$$

where b is the maximum per capita birth rate, d_i is the minimum per capita death rate in compartment i, and B and D determine the strength of the density-dependence in birth and death rates. The time delay τ reflects the duration of gestation between conception and birth.

In most temperate mammal species, births are seasonal (Macdonald 1984, Section 5.3.2.1), and this is accounted for by the function $\varphi(t)$. In wildlife management, the most common practice is to permit hunting only during a specified season, usually short compared to the rest of the year (Xu et al. 2005). This additional form of seasonality in "harvesting" is represented by the function $\psi(t)$. These two seasonality functions—$\varphi(t)$ on the birth rate and $\psi(t)$ on the harvest—are modeled by a simple periodic square function:

$$\varphi(t) = \begin{cases} 1 & \text{if } b_1 < (t \mod 1\text{year}) < b_2 \\ 0 & \text{otherwise,} \end{cases} \tag{8.42}$$

$$\psi(t) = \begin{cases} 1 & \text{if } h_1 < (t \mod 1\text{year}) < h_2 \\ 0 & \text{otherwise,} \end{cases} \tag{8.43}$$

hence, $[b_1, b_2]$ and $[h_1, h_2]$ are the periods of each year corresponding to the birth and harvest seasons, respectively, and $t \mod 1\text{year}$ is the time from the start of the year.

Although this framework is intended to be quite general, it has features that correspond closely to the dynamics of classical swine fever (CSF) disease in wild boar (Paton and Greiser-Wilke 2003). CSF is a viral disease affecting wild and domestic swine worldwide (Paton and Greiser-Wilke 2003). Outbreaks can result in severe losses in pig farms and, in Europe, wild boar populations are suspected as potential reservoirs of the disease. Moreover, wild boar populations experience wide seasonal population fluctuations due to strong density-dependent processes and harvesting. Culling of boar is considered a possibility for preventing spillover of CSF to livestock populations. In Section 8.5.1, we examine the dynamical consequences of such a strategy.

8.5.1. Equilibrium Properties

To ease analytical tractability, we initially make some simplifying assumptions, such as ignoring seasonality, using identical density-dependent terms ($B = D_X = D_W = D_Y = D_Z \equiv D$) and setting the minimum death rates to zero ($d_X = d_W = d_Y = d_Z = 0$). In addition, the maximum birth rate b is set to $2DK$ in order to give a constant carrying capacity K in the absence of harvesting and disease-induced mortality. The harvest effort and host catchability are also assumed to be independent of disease status (i.e., $H_S = H_E = H_I = H_R \equiv H$ and $q_S = q_E = q_I = q_R \equiv q$). In the absence of disease-induced mortality ($m = 0$), we can sum equations (8.36)–(8.39) to obtain a differential equation for the rate of change of the population size,

$$\frac{dN}{dt} = (b - qH)N - 2DN^2. \tag{8.44}$$

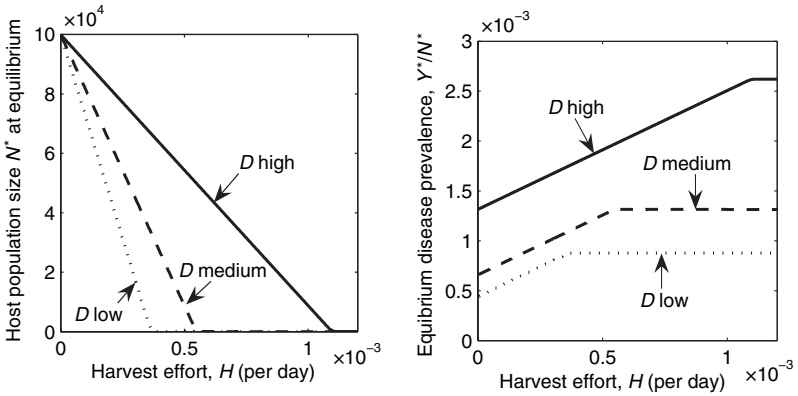

Figure 8.14. Effect of harvest effort H, on host population size N^* (left-hand graph) and disease prevalence Y^*/N^* (right-hand graph) at equilibrium, for different strengths of density dependence: $D \simeq 2.7397 \times 10^{-9}$ per day (full line), $D \simeq 1.3699 \times 10^{-9}$ per day (dashed line), and $D \simeq 9.1324 \times 10^{-10}$ per day (dotted line). The minimum per capita death rates are zero ($d_S = d_E = d_I = d_R = 0$) and the maximum birth rate b is adjusted so that the carrying capacity in the absence of harvesting is $K = 10^5$ individuals, whatever the strength of the density dependence. We thus have $b \simeq 5.4795 \times 10^{-4}$ per day (full line), $b \simeq 2.7397 \times 10^{-4}$ per day (dashed line), and $b \simeq 1.8265 \times 10^{-4}$ per day (dotted line). (Other parameter values are $q_S = q_E = q_I = q_R = 0.5$, $\beta = 5.4794$ per day, $1/\sigma = 8$ days, $1/\gamma = 5$ days and $m = 0$.)

This equation can be set to zero to obtain an equilibrium population abundance,

$$N = K - \frac{q}{2D} H, \tag{8.45}$$

which requires harvest pressure to be sufficiently small ($qH < b = 2DK$) to ensure nonnegative population equilibrium. Additionally, we can show that harvest effort H has a positive effect on the equilibrium disease prevalence Y^*/N^*:

$$\frac{Y^*}{N^*} \simeq \left(K\frac{D}{\gamma} + \frac{q}{2\gamma} H \right) \left(1 - \frac{1}{R_0} \right). \tag{8.46}$$

Not surprisingly, the equilibrium disease prevalence depends on the mean duration of the infectious period ($1/\gamma$) and the strength of density dependence (D). Given that the carrying capacity is fixed, the strength of density dependence reflects the population turnover rate, and thus the rate of susceptible recruitment, known to be a major determinant of the dynamics of diseases conferring lifelong immunity to their host (Earn et al. 2000, Chapter 2).

As harvest effort H increases, the equilibrium population size N^* decreases, but somewhat surprisingly the equilibrium disease prevalence Y^*/N^* increases (equation (8.46) and Figure 8.14, left graph). Above a harvest threshold $H^\star$, the equilibrium population size N^* reaches zero (Figure 8.14, left graph) with disease prevalence Y^*/N^* reaching its maximum $(Y^*/N^*)_{\max}$ (Figure 8.14, right graph). From equation (8.45) we can express the threshold harvest value, $H^\star = 2K\frac{D}{q}$. Substituting this into equation (8.46), we get the maximum value of the disease prevalence at equilibrium:

$$\left(\frac{Y^*}{N^*} \right)_{\max} = 2K\frac{D}{\gamma} \left(1 - \frac{1}{R_0} \right). \tag{8.47}$$

Interestingly, this means that harvesting can increase disease prevalence at equilibrium (Y^*/N^*) from its level in the absence of hunting ($KD(1-1/R_0)/\gamma$) to twice this value.

Now, if we consider the possibility of disease-induced mortality ($m > 0$), we observe a decrease in the equilibrium population size. If we sum the differential equations (8.36) to (8.39), to give an equation for the population size, N,

$$\frac{dN}{dt} = 2DKN - DN^2 - DN^2 - qHN - mY,$$

and assuming that Y is at the equilibrium value given by equation (8.46), then the population size is reduced to:

$$N^\star \approx K\left(1-\frac{m}{2\gamma}\left[1-\frac{1}{R_0}\right]\right) - \frac{q}{2D}\left(1+\frac{m}{2\gamma}\left[1-\frac{1}{R_0}\right]\right)H. \tag{8.48}$$

This is an approximation, because we have neglected the effect on the prevalence of infection of this change in the total population size. However, we expect this approximation to be reasonable unless the disease has high mortality. Equation (8.48) shows that, in the absence of harvesting, disease-induced mortality decreases the equilibrium population size by a factor of $m\xi/(2\gamma)$, where for notational convenience we set $\xi = 1-1/R_0$. However, in the presence of harvesting, disease-induced mortality mitigates the compensatory effect of density dependence by a factor of $1+m\xi/(2\gamma)$. By rewriting equation (8.48), we can tease apart all sources of mortality:

$$N^\star = K - \frac{K}{2\gamma}\left[1-\frac{1}{R_0}\right]m - \frac{q}{2D}H - \frac{q}{4\gamma D}\left[1-\frac{1}{R_0}\right]mH. \tag{8.49}$$

Thus, the total population size is reduced by the action of three elements: $Km\xi/(2\gamma)$ individuals are lost due to disease mortality, $qH/(2D)$ individuals are lost due to hunting, and $qm\xi H/(4\gamma D)$ individuals are lost due to the synergistic interaction between the disease and harvesting. Put simply, when h individuals are harvested, an additional $\frac{m\xi}{2\gamma}h$ individuals "die" from a harvest-induced increase in disease-induced mortality. Interestingly, the additional proportion of individuals dying from the disease as a side effect of harvest ($m\xi/(2\gamma)$) does not depend on the strength of the density dependence D in the host population.

8.5.2. Dynamical Properties

We now focus on model dynamics to examine the consequences of seasonality on our conclusions. At equilibrium, harvest toll on the host population cannot be more than partially compensated by density-dependent population processes—leading to damped oscillations—whereas with seasonality, it has been shown that over-compensation is possible—leading to sustained oscillations (Kokko and Lindstrm 1998; Jonzén and Lundberg 1999; Boyce et al. 1999; Xu et al. 2005). Thus, we reintroduce the seasonality functions $\varphi(t)$ (birth seasonality) and $\psi(t)$ (harvest seasonality) as well as the gestation time delay, τ. The introduction of these time-dependent terms renders the system analytically intractable, and we will thus rely on numerical simulation to explore model dynamics.

For simplicity, we will consider the infection to be benign ($m = 0$). It has been documented for a wide variety of vertebrates that density-dependent mortality is much

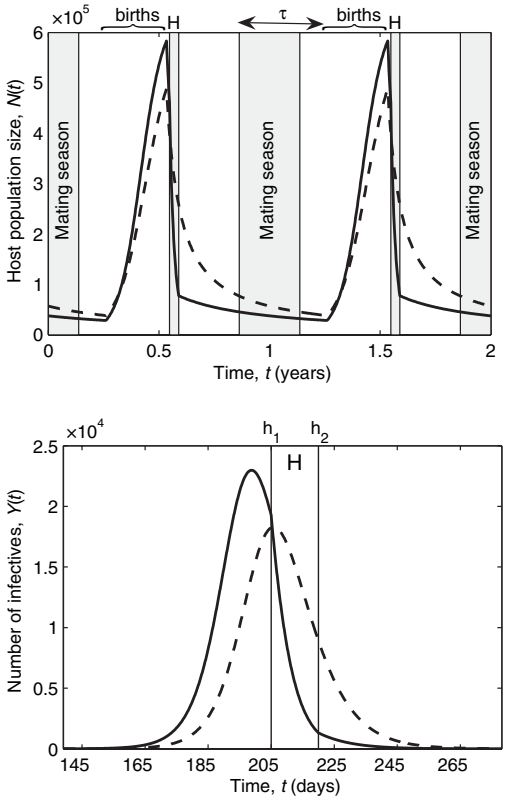

Figure 8.15. The dynamical effects of periodic harvesting and reproduction on the total host population size, $N(t)$, and the number of infected animals, $Y(t)$. The top graph shows 2 years of simulations of the model, after discarding transient dynamics. The periods of mating and harvesting (labeled H) are represented on the graph, whereas the periods of giving birth are indicated above the graph. The arrow represents the delay τ between mating and birth. The dashed curve represents the total host population size, $N(t)$, in the absence of harvesting ($H = 0$), and the full line curve represents the dynamics of the total host population size, $N(t)$, in the presence of harvesting ($H = 0.2$). The harvest season begins on day $h_1 = 205$, and ends on day $h_2 = h_1 + 15$. The lower figure shows the changes in number infected during the epidemic peak in a single year, clearly demonstrating the increase in Y as a result of harvesting (comparing solid and dashed lines). Parameter values are $K = 10^5$, $b \simeq 0.1461$ per day, $d_S = d_E = d_I = d_R = 0$, $B \simeq 4.5662 \times 10^{-7}$, $D_S = D_E = D_I = D_R \simeq 9.1324 \times 10^{-8}$, $\tau = 145$ days, $b_1 = 100$, $b_2 = 200$, $q_S = q_E = q_I = q_R = 0.5$, $\beta = 5.4795$ per day, $1/\sigma = 8$ days, $1/\gamma = 5$ days, and $m = 0$.

stronger in the younger age classes than in adults, where it is often negligible (Hudson 1992; Clutton-Brock et al. 1997; Gaillard et al. 2000). Therefore, we assume a constant mortality rate for the recovered class of individuals, which generally contains the older animals: $D_R > 0$ and $d_R = 0$.

In Figure 8.15 (top graph) we show two years of the total long-term host population dynamics with (full line) and without (dashed line) harvesting. Based on the hunting of

wild boar, the harvest season is assumed to begin 5 days after the end of the birth season and to last for 15 days. In the absence of harvesting, the host population dynamics are pronouncedly annual, driven by birth pulses. As can be seen in the window of harvesting in Figure 8.15 (top graph), hunting very quickly and dramatically reduces the number of individuals in the population, with two key consequences. First, the number $N(t-\tau)$ of individuals during the breeding season is reduced; this reduces the competition on the remaining individuals, which in turn increases the per capita birth rate ν that season (see equation (8.40)). Second, the per capita death rate is decreased (equation (8.41)), which means more females survive from mating to giving birth; in fact, N immediately prior to the birth season is very close to its size in the absence of harvesting. The combination of these two effects results in a substantial increase in the number $\nu \times N$ of individuals born. This is a clear case of overcompensation where the effect of hunting increases the host population size after the birth season. Not surprisingly, this also results in a substantial increase in disease prevalence in the population (Figure 8.15, bottom graph).

In wildlife populations subject to age-specific density dependence with an endemic pathogen, harvesting of adults can release intraspecific competitive pressure, thereby increasing the influx of susceptible juveniles. Therefore, paradoxically, attempts to reduce infection prevalence by culling can result in a dramatic increase in diseased individuals.

8.6. FUTURE DIRECTIONS

The refined control of infectious diseases is one of the key strategic uses of epidemiological modeling. To this end, models can have two main inputs. The first is to provide a better generic understanding of infectious disease transmission and control so that informed decisions can be made in the early stages of an outbreak, even before explicit models or parameters are available. The second benefit of modeling comes from creating detailed models that can make reasonably accurate predictions, and therefore allow a refinement of early control decisions and estimates of the magnitude of the epidemic and resources needed for control.

There are many particular areas of epidemiologically modeling where great progress can still be made on understanding and optimally targeting control measures.

1. For heterogeneous populations, it is still an open problem to determine the optimal deployment of control measures (e.g., vaccine, tracing effort) between risk-groups—in particular, a generic understanding of the impact of over- or under-targeting would be highly beneficial.
2. For diseases that affect multiple hosts (especially zoonotic infections), models may allow us to understand the disease behavior in the largely unsampled animal reservoir, and the implications of these dynamics for human cases. When multiple strains of a pathogen are interacting within the community, it may be possible to apply control so as to influence the competitive pressures on the strains, driving the more harmful pathogen extinct. This is particularly important for antibiotic resistant infections, where the act of control is itself a driving force for evolutionary change.
3. The fluctuations driven by seasonal forcing can also potentially be utilized by a control program, and even enhanced by tools such as pulse vaccination. It still remains

an open problem to understand how seasonal forcing and pulsed control interact, and whether this interaction can be used advantageously.

4. Similarly, control methods that enhance the risk of stochastic extinction could be used to great effect if subsequent reintroductions of infection could be controlled. The risk of such stochastic extinctions could be increased by inducing oscillatory dynamics, or by effectively subdividing the population and limiting the interaction between subgroups. It is still an open and difficult modeling exercise to assess how spatial structure or population subdivision interacts with stochasticity.
5. When dealing with spatially structured populations, there is a clear trade-off between local targeting of control measures in infected regions and the prevention of spread to new susceptible areas. Yet again, models can help in assessing the optimal balance of these two conflicting demands on resources.

Finally, one of the biggest challenges facing epidemiological modeling today is to be able to respond quickly to new and emerging infections. This not only requires the rapid development of suitable modeling tools, but also necessitates a range of sophisticated statistical methods that can uncover parameter values (and confidence intervals) from early case reports. Even determining R_0 from the first few generations of transmission is a difficult task, and prone to error. It is therefore vital that parameter estimation matches the continued development of ever more complex and parameter-rich models.

8.7. SUMMARY

In this chapter, we examined the modeling issues surrounding a number of alternative methods of disease management in different scenarios. Using simple models, we explored topics such as widespread pediatric immunization to control childhood infections, the consequences of imperfect vaccines, the role of pulse vaccination, as well as nonvaccine-related control options such as contact tracing and isolation. These models were appropriately modified to explore complexities. We examined age-related aspects of vaccination within the context of rubella, potential delays in implementing quarantine measures, and the importance of alternative assumptions concerning the distributions of latent and infectious periods when thinking about control of deliberate exposure to smallpox. The most complex and detailed model we considered was the stochastic, spatially explicit multi-pathogen framework used to study aspects of foot-and-mouth disease.

The main findings of this chapter can be summarized along the following lines:

➤ A system subject to constant long-term vaccination of a fraction p of newborns against an infection with a basic reproductive ratio R_0, with a modified per capita birth rate of μ', is dynamically equivalent to an unvaccinated population with a birth rate of μ but with $R_0' = (1-p)\frac{\mu'}{\mu}R_0$.

➤ To control a disease conforming to the assumptions of the SIR model, we can estimate the fraction of recruits into the susceptible class that need to be vaccinated to eradicate an infection: $p_c = 1 - 1/R_0$. All newborns need not be vaccinated as long as a threshold level of "herd immunity" within the population is established. Note that the critical vaccination threshold is a saturating function of R_0.

➤ When a fraction p of infants are vaccinated, the mean age at infection increases by a factor $\frac{1}{1-p}$.

➤ When vaccination is aimed at the susceptible population in general (and not newborns), the critical *rate* of vaccination for effective control is $p_c \geq \mu(R_0 - 1)$. Note that this scales linearly with R_0.

➤ Eradication with an imperfect vaccine, subject to incomplete protection and loss of vaccine-induced immunity, is much more difficult. If the vaccine is 100% protective, eradication requires the mean period of protection afforded by the vaccine to exceed the average life expectancy by a factor $1 - 1/R_0$.

➤ Pulse vaccination of susceptibles is an alternative approach to controlling infections. For any specific infection and host demographic traits, it is possible to derive the relationship between the pulse vaccination level (p_V) and the optimal pulsing period (T_c).

➤ Age-specific considerations point toward a focus on the very young ages in order to exert strongest control. This argument is strongly affected by complicating factors such as transplacentally derived antibodies.

➤ Age-specific complications of infection (as exemplified by rubella) can affect the aims of a public health program. In such situations controls will be aimed at reducing the level of disease (or severe symptoms), rather than simply reducing the total prevalence of infection.

➤ Targeted vaccination can be incorporated into models in order to highlight the differential effort that needs to be concentrated on high-risk groups before attention is turned to lower- risk categories.

➤ In simple models, it is possible to derive levels of isolation and quarantine practices needed for infection control during an epidemic. The addition of realistic complexities highlight the need for additional controls such as targeted and ring vaccination.

➤ The assumptions made concerning the distribution of latent and infectious periods is shown to be very important when making quantitative predictions.

➤ Using foot-and-mouth disease as a case study, the role of a large number of epidemiological and ecological complexities, in addition to alternative control options, are addressed. In particular, we have seen how effective control can be locally targetted when transmission is a spatial process.

➤ Examining the dynamics of swine fever in wild boar populations has highlighted how multiple seasonal factors can interact to produce complex and often counter-intuitive behavior.

Throughout this chapter we have seen how the understanding from simple tractable models can be extended to more applied senarios. Although the addition of extra realism generally involved a substantial increase in the number of parameters (which need to be estimated), such models are vital if modelers are to provide informed and accurate predictions.

This page intentionally left blank